(2)

FJSRL TR-91-0001

FRANK J. SEILER RESEARCH LABORATORY

DOWNWASH MEASUREMENTS ON A PITCHING CANARD - WING CONFIGURATION

JOHN E. BURKHALTER

SEPTEMBER 1991

AIR FORCE SYSTEMS COMMAND

UNITED STATES AIR FORCE

FJSRL-TR-91-0001

This document was prepared by the Aerospace Sciences Division, Frank J. Seiler Research Laboratory, United States Air Force Academy, CO. The research was conducted under Project Work Unit Number 2307-F1-38, Unsteady Airfoil Energized Flow. Dr John E. Burkhalter was the Project Scientist in charge of the work.

When U.S. Government drawings, specifications or other data are used for any purpose other than a definitely related government procurement operation, the government thereby incurs no responsibility nor any obligation whatsoever, and the fact that the government may have formulated, furnished or in any way supplied the said drawings, specifications or other data is not to be regarded by implication or otherwise, as in any manner licensing the holder or any other person or corporation or conveying any rights or permission to manufacture, use or sell any patented invention that may in any way be related thereto.

Inquiries concerning the technical content of this document should be addressed to the Frank J. Seiler Research Laboratory (AFSC), FJSRL/NA, USAF Academy, CO 80840-6528. Phone (719) 472-2812.

[This report has been reviewed by the Commander and is releasable to the National Technical Information Service (NTIS). At NTIS it will be available to the general public, including foreign nations.]

This technical report has been reviewed and is approved for publication.

John E. Burkhalter
JOHN E. BURKHALTER, PhD
Research Associate

Richard W. Newsome Jr.
RICHARD W. NEWSOME, Jr., Lt Col, USAF
Chief, Aerospace Sciences Division

Barry G. Morgan
BARRY G. MORGAN, Lt Col, USAF
Commander

REPORT DOCUMENTATION PAGE

Form Approved
OMB No 0704-0188

1. AGENCY USE ONLY (Leave blank)	2. REPORT DATE	3. REPORT TYPE AND DATES COVERED
	15 Sep 91	Final (16 Jun 90–15 Sep 91)

4. TITLE AND SUBTITLE

Downwash Measurements on a Pitching Canard – Wing Configuration

5. FUNDING NUMBERS

2307–F1–38

6. AUTHOR(S)

John E. Burkhalter

7. PERFORMING ORGANIZATION NAME(S) AND ADDRESS(ES)

Frank J. Seiler Research Laboratory
USAF Academy CO 80840–6528

8. PERFORMING ORGANIZATION REPORT NUMBER

FJSRL–TR–91–0001

9. SPONSORING/MONITORING AGENCY NAME(S) AND ADDRESS(ES)

10. SPONSORING/MONITORING AGENCY REPORT NUMBER

11. SUPPLEMENTARY NOTES

12a. DISTRIBUTION/AVAILABILITY STATEMENT

Distribution Unlimited

12b. DISTRIBUTION CODE

13. ABSTRACT *(Maximum 200 words)*

A series of experimental wind tunnel tests were conducted using a splitter plate model of a two wing configuration oscillating through an unsteady pitch maneuver. Of primary interest were measurements of circulation lag on each wing and the downwash on the aft wing due to the forward wing. It was found that circulation lag associated with oscillating wings is independent of external induced downwash flow fields but is dependent on the location of the pivot point for the wing or airfoil section, the starting and ending angle, and the angle of attack history. Downwash from a forward wing on an aft lifting surface can make a significant contribution to the lifting properties of the aft wing. The magnitude of these downwash forces are dependent on the forward wing normal force magnitudes and may enhance or degrade the potential of an aft wing to produce lift. The downwash induced in this case, however, is not synchronized with the circulation lag associated with the forward wing but the shift in the downwash curve is more or less synchronized with the circulation lag associated with the aft wing. Consequently a forward wing producing positive lift can produce upwash on an aft wing increasing its potential to produce lift. Enhancement of maneuverability for an aircraft can also be increased by placing the forward canard above the main wing lifting surface.

14. SUBJECT TERMS	15. NUMBER OF PAGES
Unsteady aerodynamics; Downwash; Canards; Circulation; Time lag; Experimental Data	72
	16. PRICE CODE

17. SECURITY CLASSIFICATION OF REPORT	18. SECURITY CLASSIFICATION OF THIS PAGE	19. SECURITY CLASSIFICATION OF ABSTRACT	20. LIMITATION OF ABSTRACT
UNCLASSIFIED	UNCLASSIFIED	UNCLASSIFIED	NONE

GENERAL INSTRUCTIONS FOR COMPLETING SF 298

The Report Documentation Page (RDP) is used in announcing and cataloging reports. It is important that this information be consistent with the rest of the report, particularly the cover and title page. Instructions for filling in each block of the form follow. It is important to **stay within the lines to meet optical scanning requirements.**

Block 1. Agency Use Only (Leave Blank)

Block 2. Report Date. Full publication date including day, month, and year, if available (e.g. 1 Jan 88). Must cite at least the year.

Block 3. Type of Report and Dates Covered. State whether report is interim, final, etc. If applicable, enter inclusive report dates (e.g. 10 Jun 87 - 30 Jun 88).

Block 4. Title and Subtitle. A title is taken from the part of the report that provides the most meaningful and complete information. When a report is prepared in more than one volume, repeat the primary title, add volume number, and include subtitle for the specific volume. On classified documents enter the title classification in parentheses.

Block 5. Funding Numbers. To include contract and grant numbers; may include program element number(s), project number(s), task number(s), and work unit number(s). Use the following labels:

C	- Contract	**PR**	- Project
G	- Grant	**TA**	- Task
PE	- Program Element	**WU**	- Work Unit Accession No.

Block 6. Author(s). Name(s) of person(s) responsible for writing the report, performing the research, or credited with the content of the report. If editor or compiler, this should follow the name(s).

Block 7. Performing Organization Name(s) and Address(es). Self-explanatory.

Block 8. Performing Organization Report Number. Enter the unique alphanumeric report number(s) assigned by the organization performing the report.

Block 9. Sponsoring/Monitoring Agency Names(s) and Address(es). Self-explanatory.

Block 10. Sponsoring/Monitoring Agency. Report Number. (If known)

Block 11. Supplementary Notes. Enter information not included elsewhere such as: Prepared in cooperation with...; Trans. of ..., To be published in .... When a report is revised, include a statement whether the new report supersedes or supplements the older report.

Block 12a. Distribution/Availablity Statement. Denote public availability or limitation. Cite any availability to the public. Enter additional limitations or special markings in all capitals (e.g. NOFORN, REL, ITAR)

DOD - See DoDD 5230.24, "Distribution Statements on Technical Documents."
DOE - See authorities
NASA - See Handbook NHB 2200.2.
NTIS - Leave blank.

Block 12b. Distribution Code.

DOD - DOD - Leave blank
DOE - DOE - Enter DOE distribution categories from the Standard Distribution for Unclassified Scientific and Technical Reports
NASA - NASA - Leave blank
NTIS - NTIS - Leave blank.

Block 13. Abstract. Include a brief (Maximum 200 words) factual summary of the most significant information contained in the report.

Block 14. Subject Terms. Keywords or phrases identifying major subjects in the report.

Block 15. Number of Pages. Enter the total number of pages.

Block 16. Price Code. Enter appropriate price code (NTIS only).

Blocks 17. - 19. Security Classifications. Self-explanatory. Enter U.S. Security Classification in accordance with U.S. Security Regulations (i.e., UNCLASSIFIED). If form contains classified information, stamp classification on the top and bottom of the page.

Block 20. Limitation of Abstract. This block must be completed to assign a limitation to the abstract. Enter either UL (unlimited) or SAR (same as report). An entry in this block is necessary if the abstract is to be limited. If blank, the abstract is assumed to be unlimited.

TABLE OF CONTENTS

LIST OF FIGURES

LIST OF SYMBOLS

Symbol	Description
c_l	Sectional lift coefficient
c_{l_α}	Sectional lift curve slope; $dc_l/d\alpha$
C_N	Normal force coefficient
C_{N_α}	Sectional normal force coefficient slope; $dC_N/d\alpha$
α	Angle of attack
α_{ss}	Steady state angle of attack
ϵ	Downwash
t	Time
z	Vertical displacement
q	Pitch rate
Ω	Reduced frequency; Eqs. (7) and (8)
f	Harmonic frequency; Eqs. (7) and (8)
c	Chord length
V_∞	Free stream velocity
R_f	Reduced frequency; Eq. (9)
r_{LE}	Distance from pivot point to wing leading edge
ω	Harmonic frequency; Eq. (9)
θ	Splitter plate angle (angle of attack)
CNA	Normal force coefficient for aft balance; $N/(q_\infty S)$
CMA	Moment coefficient for aft balance; $M/(q_\infty Sc)$
CLLA	Aft root chord bending moment coefficient; $M/(q_\infty Sc)$
XAC	Chordwise center of pressure for aft wing
CNB	Normal force coefficient for fwd balance; $N/(q_\infty S)$
CMB	Moment coefficient for fwd balance; $M/(q_\infty Sc)$
CLLB	Fwd root chord bending moment coefficient; $M/(q_\infty Sc)$
XBC	Chordwise center of pressure for fwd wing
DCNA	Delta normal force coefficient due to downwash
DCMA	Delta moment coefficient due to downwash
DCLA	Delta root chord bending moment due to downwash
DXCA	Delta change in chordwise center of pressure due to downwash

INTRODUCTION

Background

It has long been known that oscillating airfoils or wings can produce normal forces and pitching moments which exceed the normal static aerodynamic limits. That is, if an airfoil section is pitched at some cyclic rate, then the measured normal force at stall is considerably higher than the static limit[1]. The stall angle for the oscillating case may be more than double the static stall angle of attack and the mechanics of the stall is indeed different from the static case. Several researchers have investigated the stall mechanism and there appears to be a difference of opinion as to the actual fluid mechanics of the stall. Two descriptions of the stall will be discussed here and one can note the similarities and differences.

Carr, in Ref. 1, describes the stall for a two-dimensional airfoil section specifically related to a helicopter blade. It was observed that "...as the airfoil continues to pitch upward, a point is reached where a surge in the lift force and negative roll-off in pitching moment occurs. Simultaneously, a vortex can be seen to grow and be shed from the leading-edge region." This vortex moves back over the airfoil surface causing an increase in lift and a further decrease in the pitching moment.

With this description of vortex movement over the airfoil surface, logic would lead one to believe that the leading edge vortex tends to act as a mechanism for keeping the flow attached at least for the forward portion of the airfoil surface. The final "stall", as described in Ref. 1 and again in Ref. 2, occurs when the vortex finally moves past the trailing edge causing a sudden loss in lift exhibited as a sharp break in the C_L-alpha curve. Because of the movement of the vortex over the airfoil surface, the sudden loss in lift is not coincident with the sudden change in pitching moment about the quarter chord. Consequently, the "moment" stall has been distinguished from the "lift" stall.

The second description of the stall mechanism is presented in Ref.3. Conclusions in this report were drawn from flow visualization using a smoke wire-strobe arrangement accompanied by pressure measurements made on the airfoil surface. In this paper, it was observed that a leading edge vortex first appears on the upper surface of the airfoil at the beginning of the stall sequence. The vortex first grows in an elongated manner along the surface of the airfoil during which time the lift continues to increase. As the vortex passes over the 25 to 30 percent chord point, the vortex begins to grow in a direction normal to the airfoil surface and becomes more circular in the process. Just prior to this circular growth, lift reaches a maximum and continues to decrease as the vortex moves away from the airfoil into the free stream but not necessarily at the airfoil trailing edge. Consequently, the stall seems to be associated with the onset of rapid growth of the vortex

perpendicular to the airfoil surface and not with the movement past the trailing edge as indicated in Ref. 1.

The question logically arises as to whether the two descriptions of dynamic stall discussed in Ref. 1 and Ref. 3 can be reconciled. From both descriptions, the lifting properties of the airfoil section are related to the initiation of a leading edge vortex and the stall, in some manner, is associated with the shedding of vorticity from the airfoil surface. The differences may possibly be attributed to the airfoil shape but more likely to the "motion" of the airfoil itself. That is, the motion history of the airfoil can significantly alter the loading properties of the airfoil section. If the airfoil starts from an angle of attack of 0.0 and is cycled sinusoidally through some arc and back to zero, the measured loads and moments will be different from a case where the airfoil starts from an angle of attack of -30 degrees then cycled sinusoidally through the same arc. If the motion is a "ramp" motion instead of a sinusoidal motion, the loading may be different. Therefore, the motion history of an airfoil section is an important factor to consider when describing details of the stall mechanism.

In Ref. 4, the dynamic stall is discussed in terms of the relative location of the pitch axis. When the pitch axis is moved from points in front of the leading edge to the quarter chord, to points aft of the trailing edge, the stall angle increases to larger and larger values. Yet, present studies indicate differing results as will be discussed in a later section. Why are there so many differences in results in unsteady flow experiments? The reason, again, is attributed to the motion history of the airfoil section as well as similarity matching problems.

From a three-dimensional viewpoint, a wing undergoing a pitching motion should exhibit similar characteristics to a two-dimensional airfoil section. However, one would expect the "moment" stall, as discussed in Refs.1 and 2, to be masked by "multiple stalls" along the span of the lifting surface since the chordwise movement of the shed vortices would not occur simultaneously for all spanwise stations. The flow field for the three-dimensional case is further complicated by trailing vortices in the streamwise direction creating induced velocities from the vortex trailing legs. Nevertheless, a significant increase in lift and pitching moments is observed for finite lifting surfaces as shown in Ref. 5.

Time Lag and Motion Histories

The transition in thinking from steady state analysis to the unsteady case requires that several key elements be taken into account. As pointed out in Ref. 6, there is a time lag in the transition of aerodynamic loads and moments during cyclic pitching and/or translation of airfoil sections. For the case of a pitching airfoil section (or wing) about some arbitrary pivot point not on

the airfoil, the analysis may be broken down into a pure translation and pure pitch. This, of course, is true only if linear aerodynamics is assumed. The sectional normal force coefficient, as a function of time, is then

$$c_l(t) = c_l(\alpha_{ss}) + c_{l_\alpha}\,\alpha_{translation} + c_{l_q}\,\alpha_{rotation} \tag{1}$$

Using similar reasoning, the same can be said of finite wings and therefore

$$C_N(t) = C_N(\alpha_{ss}) + C_{N_\alpha}\,\alpha_{translation} + C_{N_q}\,\alpha_{rotation} \tag{2}$$

For the three-dimensional case, the first term on the right hand side of Eq. (2) represents the steady state normal force coefficient as measured or predicted by a variety of theories. The second term represents the contribution to the normal force due to translation of the wing and the third term represents the contribution due to rotation. As outlined in Ref. 6, the effective angle of attack due to translation of the wing vertically may be characterized by two terms, one attributed to the velocity in the vertical direction, dz/dt, and the other due to self induced downwash.

$$\alpha_{translation} = \alpha(dz/dt) + \alpha(\epsilon) \tag{3}$$

The downwash term may be further broken down into three separate contributions. The first is the induced flow due to the velocity in the vertical direction, dz/dt, the second is the induced downwash due to trailing vortex legs, and the third is due to shed vorticity caused by changing loads on the wing surface as a function of time. That is

$$\alpha(\epsilon) = \alpha[\epsilon(dz/dt)] + \alpha[\epsilon_i] + \alpha[\epsilon_i\,(t-\Delta t)] \tag{4}$$

where ϵ_i is the steady state induced downwash due to vortex trailing legs. The third term on the right in Eq. (4) is present in two-dimensional flows as well as three-dimensional flows and is due to vortices created near the wing leading edge and then shed over the wing surface and off the trailing edge as described in Refs. 1-3. The downwash induced on the wing due to these vortices is felt by the wing on a "delayed" basis since their strength is due to the rate at which the wing loading is changing in time. Hence, this downwash contribution creates a lag in the loading measured on the wing and appears as a lag in the physical measurement of angle of attack.

Finally, one last term must be added to Eq. (4) in order to complete the system. This last term is also due to downwash in the flow but is not self induced.

$$\alpha(\epsilon) = \alpha[\epsilon(dz/dt)] + \alpha[\epsilon_1] + \alpha[\epsilon_1 (t-\Delta t)] + \alpha[\epsilon_e (t-\Delta t)] \qquad (5)$$

The last term on the right of Eq.(5) represents the time dependent downwash in the flow field due to external lift producing devices, usually an additional wing, canard, fin, or body.

Returning to Eq. (2), the last term on the right represents the normal force contribution due to pure rotation of the wing or airfoil about the quarter chord. The angle of attack associated with the rotation of the wing can be subdivided into a contribution due to pitch rate and a contribution due to downwash. That is

$$\alpha_{rotation} = \alpha[q(t)] + \alpha\{q[\epsilon_1 (t-\Delta t)]\} + \alpha_c [q(t-\Delta t)] \qquad (6)$$

The last term on the right hand side of Eq. (6) is the contribution to alpha due to the fact that the leading edge and trailing edge of the wing are not moving in the same direction (up/down) and therefore "creates" an apparent camber not physically present. This in fact causes the chordwise load distribution to change which may not necessarily be synchronized with the sinusoidal unsteady motion of the wing and consequently is "felt" on a delayed basis. Actual camber terms are included in the steady state terms of Eq. (2).

If the normal force for a finite lifting surface is treated as a spanwise integration of the sectional circulation, then resulting measured loads for an oscillating, pitching wing appear as a circulation lag in normal force measurements, as discussed in Ref. 6, for two-dimensional flows. The circulation, for a finite wing, is characterized by the "bound" vorticity and the shed vorticity which in the unsteady case is not of equal strength at some given instant in time. Consequently, one would expect in experimental tests of finite wings, that the aerodynamic loading curves would not conform to "standard" shapes. The circulation lag or the lag in the normal force coefficients should be viewed as a shift in the loading curves and not as a shift in angle of attack. However, it is convenient to view the situation as a lag in alpha and this approach seems to be justified as noted in Eqs. (5) and (6).

Additional Apparent Lags

Because of the shifting position of flow separation lines and subsequent regions of accelerated flow, the shape of the "normal" aerodynamic load and moment curves becomes altered. The sagging or rising of sections of these curves shows up as a "lag" between the steady and unsteady cases due, in part, to accelerated regions in the flow. This particular problem may be even more pronounced when additional lifting surfaces are introduced into the flow; however, little quantitative information is available for comparison purposes. In wind tunnel applications, wall effects may become more important in unsteady applications since local regions of accelerated flow due to unsteady constricting streamlines may become a factor. Finally, the fact that the boundary is moving in the unsteady case requires that unsteady boundary conditions be considered.

Summary

In Ref. 6, Ericsson and Reding provide a structured approach to the problems associated with a theoretical analysis. The various terms in the force and moment equations are discussed along with a two-dimensional solution for simple harmonic motion. Prediction of phase angles, due to circulation lag, of about 15 degrees for specific configurations seems to be typical. Ericsson and Reding also discuss scaling problems and similarity matching in Ref. 7, pointing out that Reynolds number and Mach number simulation can conflict with a reduced frequency simulation for subscale tests. Because of the apparent scaling conflicts associated with dynamic testing, as pointed out in Ref. 7, it would seem that full-scale Reynolds number, and perhaps Mach number, would be an essential requirement for obtaining quantitative data. This, however, is not the case and Ericsson and Reding point out that considerable insight can be gained in unsteady aerodynamics by using subscale steady-state data coupled with judicious unsteady formulations extrapolated into the unsteady regime. Short of full-scale Reynolds number and Mach number testing with full-scale authentic models at real-time maneuvering rates, subscale tests can still lend significantly to our database of knowledge. An intermediate step between these two extremes is subscale testing of realistic models, such as presented in Refs. 8, 9, and 10, or theoretical modeling of full-scale configurations as attempted in Refs. 11 and 12.

Downwash

Much of the experimental work associated with unsteady flows has centered around the harmonic oscillations of a single lifting surface, usually rotated about the quarter chord, and the

resulting changes in the flow field surrounding the model[13,14]. Only a few investigations[15,16] have considered the translation and rotation of finite wings such as encountered on real, full-size, fighter type, supermaneuverable aircraft in deep stall. Yet aircraft of this type are flying, though perhaps designed by wind tunnel experiments and empirical means. In spite of the success in the design of such aircraft, as noted in Ref. 2, theoretical prediction of unsteady performance of rigid and elastic dynamics of real aircraft in deep stall is still several years away. Probably the best summary of the state of the art using a theoretical approach is found in Refs. 6, 7, and 11.

In only a few investigations has the concept of downwash from external lifting surfaces been discussed at all and none has placed a major emphasis on its importance. Perhaps the reason for such an omission is the fact that so little is really understood about much simpler configurations and a more complex model involving two or more lifting surfaces would not lend itself to very much additional insight into the physics of the unsteady flowfield. However, most supermaneuverable aircraft employ a forward and aft lifting surface and most assuredly the downwash is important.

Consider, now, the loading on a lifting surface during a simple unsteady pitch maneuver. If one now places an additional wing in the downstream oscillating wake of the upstream lifting surface, what kind of loads will be experienced by the aft wing surface due to the presence of the forward lifting surface? One could also ask, what changes in loads and moments will be experienced by the forward wing due to the "oscillating" aft wing? Since the two wings are separated fore and aft by a finite distance, the rotation point is not at the quarter chord of either wing. It was shown in Ref. 17 that the maximum lift coefficient experienced during sinusoidal oscillation changes drastically with alterations of the lifting surface rotation point. For the two-wing case, with the rotation point somewhere between the two wings, one would expect significant deviations from the quarter chord rotation point data. If the two wings are separated in the vertical direction, simulating a high wing and low tail or a low canard and high wing combination, what changes would be expected in the loading and moments on each wing/canard/tail? Suppose the wing and/or tail is rotated through a finite dihedral angle or suppose the span on the wing or tail is increased or decreased, what changes would be expected in the loads and moments?

The answer to these questions could be inferred from steady-state theory and assumptions as to the vortex structure in the unsteady case, but definitive, quantitative answers are difficult to obtain from both a theoretical and experimental approach. Since an answer to most of the inherent questions is not immediately predictable from theory, it seems prudent to try and identify qualitatively (and quantitatively) the essential features of the resulting flow field for the two-wing case in a manner that does not require full-scale Reynolds number or Mach number simulation. One such study was completed by Walker[18] in which a forward two-dimensional airfoil was pitched about its quarter chord axis at a constant rate. Flow visualization results indicated that the leading edge

vortex, separated from the forward airfoil section, could be made to pass either over or under the aft airfoil. Results from the tests by Walker indicate that loads produced by the forward wing "...produce serious effects to aerodynamic bodies passing in the immediate wake of airfoils generating unsteady vortex structures." In these experiments, the Reynolds number was very low and the Mach number was essentially zero.

In some cases, such as those described in Ref. 18, the downwash loading from forward lifting surfaces can make significant contributions to the loading on a downstream wing or tail. Because downwash loads and moments are difficult to predict theoretically, especially for unsteady motions, a series of wind tunnel tests were completed in a low speed wind tunnel on a generic configuration as pictured in Figs. 1 - 3, in which attempts were made to measure downwash directly.

Downwash measurements may take the form of localized induced flow velocities or globally as changes in the "normal" aerodynamic coefficient. It is much easier to measure changes in the aerodynamic coefficients than to measure three-dimensional velocity components in an unsteady flow field although these measurements could certainly be made. For the present experiments, the changes in loads and moments on a particular wing of interest due to the downwash field were measured as opposed to localized downwash velocities.

Reduced Frequency

At the outset, one of the major contributors to aerodynamic loading on a two-fin configuration would be the relative rotation rate. If one views the rate as being cyclic in nature, then, as several authors have done, a reduced frequency can be defined. However, the definition of the reduced frequency is open to one's own preference. There are two basic definitions currently in use and differ only by a factor of 2.0 in the denominator.

$$\Omega = fc/V_\infty \tag{7}$$

or

$$\Omega = fc/(2V_\infty) \tag{8}$$

In Refs. 6, 7 and 17, Eq. (7) is used as the definition of the reduced frequency and in Refs. 1, 10, and 13-16, Eq. (8) is employed. Obviously there is no consensus as to the definition. However, in Ref. 17, it is pointed out that Eq. (7) is simply the inverse of the Rossby number associated with long (atmospheric) wave analyses. In the present paper, it is proposed that the definition of the reduced frequency be the ratio of the rotational velocity of the leading edge of the wing or airfoil

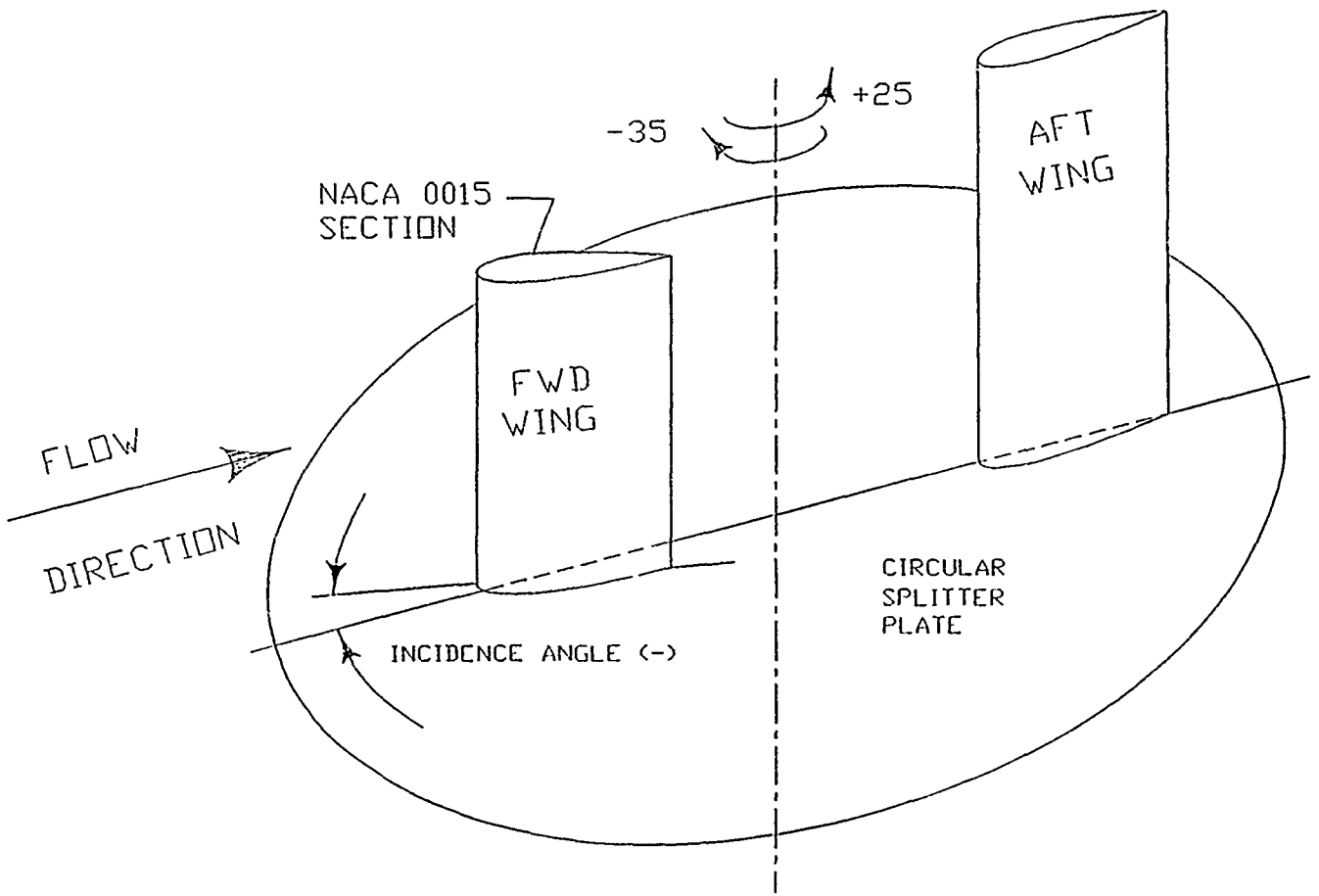

Fig. 1. Schematic of Splitter Plate Model

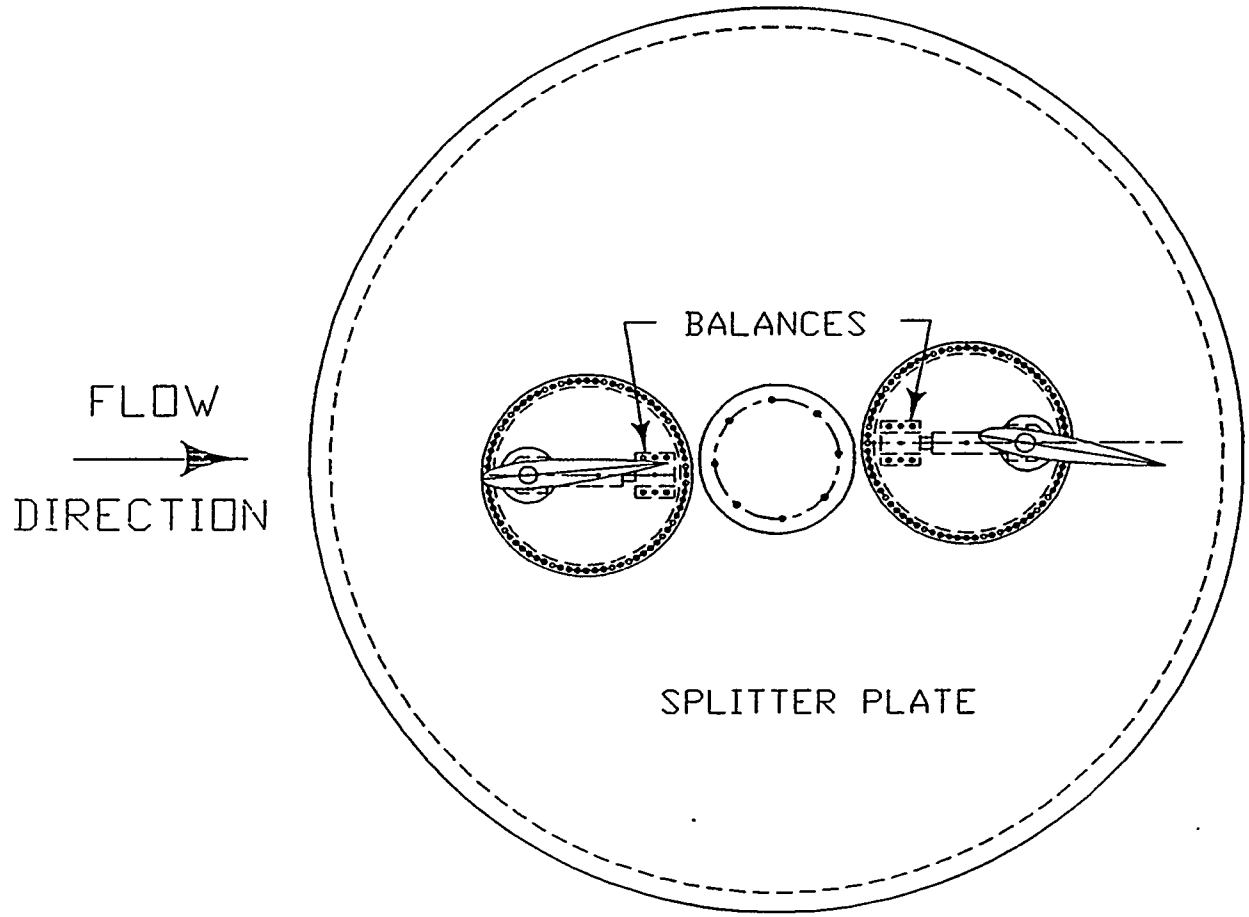

Fig. 2. Top View of Splitter Plate and Wing Assembly

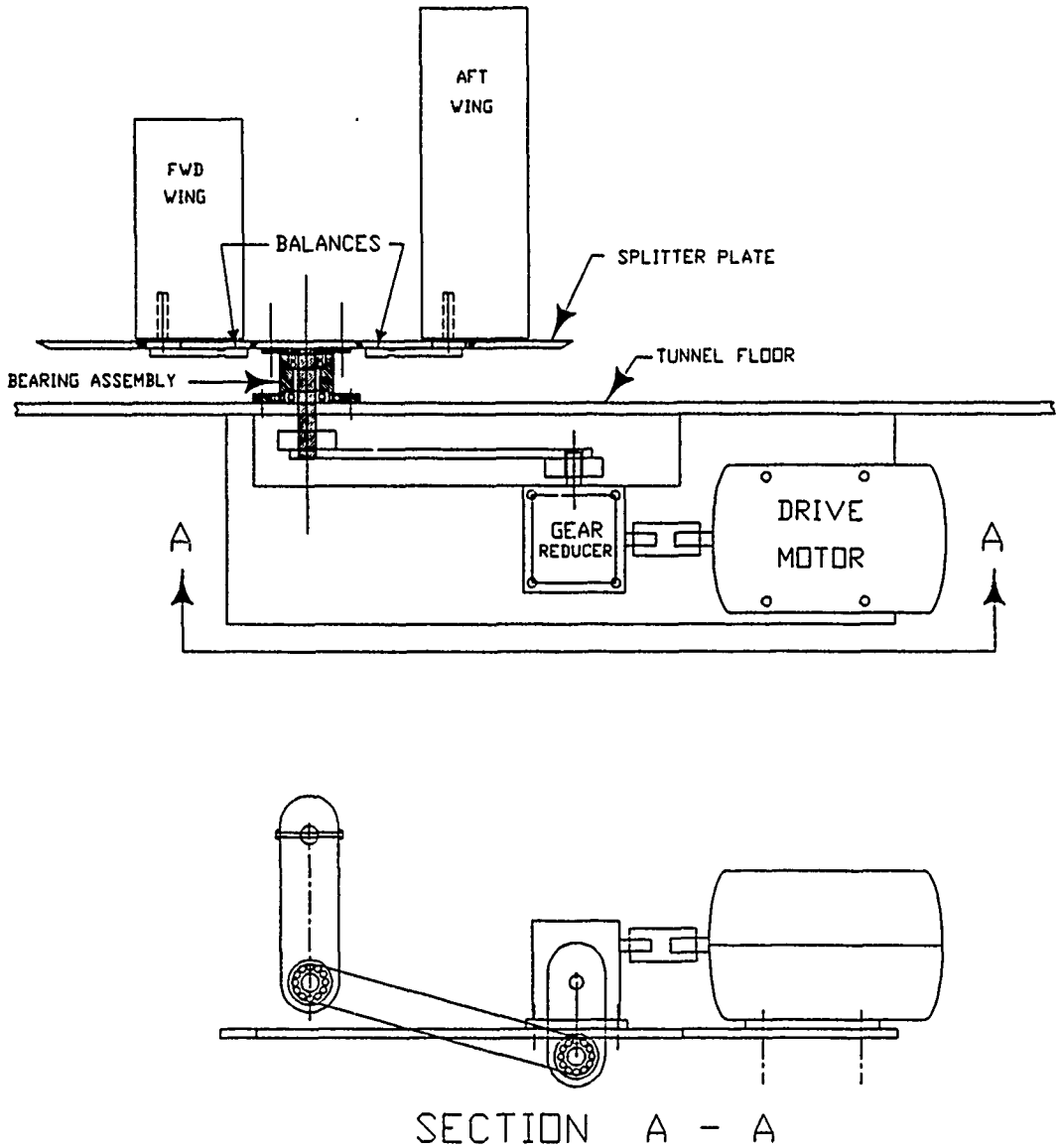

Fig. 3. Sideview of Splitter Plate, Wing Assembly, and Drive Motor Assembly

section to the free stream velocity. That is

$$R_f = (r_{LE}\,\omega)/V_\infty \tag{9}$$

where ω is the harmonic frequency of the wing or airfoil section. For the case where the rotation point on the airfoil is at the mid chord of the airfoil, then Eq. (9) becomes identical to Eq.(8) and for the case where the rotation point is at the trailing edge, Eq. (9) becomes identical to Eq.(7). If the rotation is not sinusoidal or very near sinusoidal, then none of the definitions described above would suffice. Equation (9) could be used if the definition of ω was the instantaneous rotation rate of the leading edge (rad/sec) and not the global sinusoidal frequency.

Certainly, if one wishes to compare data from one experiment to another, the definition of R_f and ω must be the same. In the same sense, if one wishes to use the reduced frequency as a similarity parameter, then the proposed definition of Eq. (9) or something comparable must be used or Ericsson, Ref. 6, is indeed correct in implying a conflict between Reynolds number, Mach number and reduced frequency simulations.

From this discussion, the question naturally arises as to what the reduced frequency actually refers to. It appears that it has been utilized because of the assumption of harmonic or ramp motion and not necessarily as a direct consequence of unsteady motion in general. What the reduced frequency actually does for the experimenter is to provide a means of identifying the angle of attack histories of differing experiments. Cook, in Ref. 19, has shown that the nondimensional reduced frequency enters the problem through the boundary conditions since it is not a natural nondimensional variable in the equations of motion and for two experiments to be similar, the angle of attack time histories must be the same. That is, for an experiment with some reference length, C_1, and some free stream velocity, V_1, the angular history of a new experimental setup (2) must be related as

$$\alpha_2(t) = \alpha_1(\hat{\omega}\,t) \tag{10}$$

where

$$\hat{\omega} = (C_2\,V_1)\,/\,(C_1\,V_2) \tag{11}$$

For example, if two experiments were performed at the same free stream velocity, then the angle

of attack time histories must be related through their reference lengths for similarity matching. Using Eq. (9) as the definition of reduced frequency, the reference length, r_{LE}, in Eq. (9) and C_1 and C_2 in Eq. (11) should be the distance from the pivot point to the leading edge of the airfoil or wing. For wings which are swept or have dihedral and other wing "deformations", the reference length should be the distance from the pivot point to the leading edge of the mean aerodynamic chord. This implies that the Reynolds number reference length should also be changed for similarity conditions to be met. Finally, then, if Eq. (9) is used as the definition of reduced frequency and Cook's conditions for similarity are met, then data from full-scale tests may indeed be compared with subscale wind tunnel test results.

DESCRIPTION OF EXPERIMENT

The experimental wind tunnel tests were conducted in a low speed open return wind tunnel. The test section was 3' x 3' (91.44 x 91.44 cm) and the nominal free stream velocity was 89 ft/sec. producing a Reynolds number of about 2.05×10^5 based on the wing chord length of 6.0 inches. Appendix I contains a list of the configurations tested including assigned run numbers. All airfoil sections were NACA 0015 mounted to individual load and moment balances at the quarter chord.

Model and Drive Assembly

Two wing assemblies were mounted to an oscillating splitter plate connected to a shaft and bearing assembly in the floor of the wind tunnel test section. The wings were mounted in the vertical direction for ease of construction and ready access to the drive assembly underneath the tunnel floor (see Fig. 3.) The round splitter plate was beveled to a 30 degree angle to reduce boundary layer and hardware interference in the test data. Each wing was actually mounted to individual load and moment balances through a shaft along the quarter chord of each wing as illustrated in Fig. 3. This shaft, running through the quarter chord of each wing, also served as a means of setting each wing incidence angle. The bottom of each shaft was fixed to a rigid plate bolted directly to the face of each balance and the plate was designed so that its upper surface was flush with the splitter plate surface. A small gap between the root or bottom end of the wing raised the wing to near the edge of the boundary layer on the oscillating plate. A top and side view of the entire assembly is shown in Figs. 2 and 3.

The splitter plate was rigidly connected to a drive shaft supported by a large bearing assembly attached to the bottom of the tunnel. The drive shaft protruded through the bearing assembly and through the tunnel floor. The drive motor assembly consisted of a 1.0 HP variable

speed DC motor connected to a gear reducer via a flexible coupling. The output of the gear reduction unit was connected to a flywheel type connecting arm assembly which was rigidly attached to the output shaft protruding through the tunnel floor. The linkage system was so designed that one full revolution of the gear reduction output arm produced a 60 degree swing in the splitter plate. Because of the design dimensions, the plate rotation was limited to about +25 degrees and -35 degrees.

The resulting oscillation of the splitter plate assembly was near sinusoidal but not a true sine wave. Fig. 4 is a plot of typical measured rotation cycles as compared to a true sinusoidal oscillation. As can be seen from Fig. 4, the wave form is more or less sinusoidal, at least for angles greater than -10 degrees. It should be pointed out here that the experimental rotation rates were obtained by numerical differentiation of the time and angle measurements and consequently one would expect "some" scatter in the results.

Data Acquisition

Sensors for the experiment consisted of two five-component load balances, a bridge circuit assembly for the angle measurements, the tunnel speed transducer, and an optical encoder. Only three components on each balance were used consisting of normal force, pitching moment, and rolling moment (root chord bending moment). The bridge circuit was used to measure the angular position of the plate and the optical encoder was used to "start" the measuring cycle at a precise location of the splitter plate.

A high speed computer digitized each channel of data at a rate of 1.0×10^6 samples per second and stored the data in memory for later processing. Clock pulses were generated internally to the computer to start each "burst" of data at predetermined time steps during each cycle. At each clock pulse, each channel was sampled four times at the 1.0 M Hz. rate. Each data cycle was repeated four times to produce aggregate data which was averaged in order to eliminate "some" of the scatter in the data and to eliminate "some" of the electronic noise. The data were also electronically filtered using a low pass filter to further eliminate electronic noise. Clock pulse frequencies were adjusted to correspond to approximately 30 data sets (angular positions of the splitter plate) depending on the preset rotation rate of the drive motor. It was assumed that the clock pulses occurred at the same angular positions of the splitter plate during each of the four cycles so that data from each cycle could be averaged. After all data from each cycle was stored in memory, post processing of the data produced final coefficients, numerically differentiated angular velocities, and corrected angular positions.

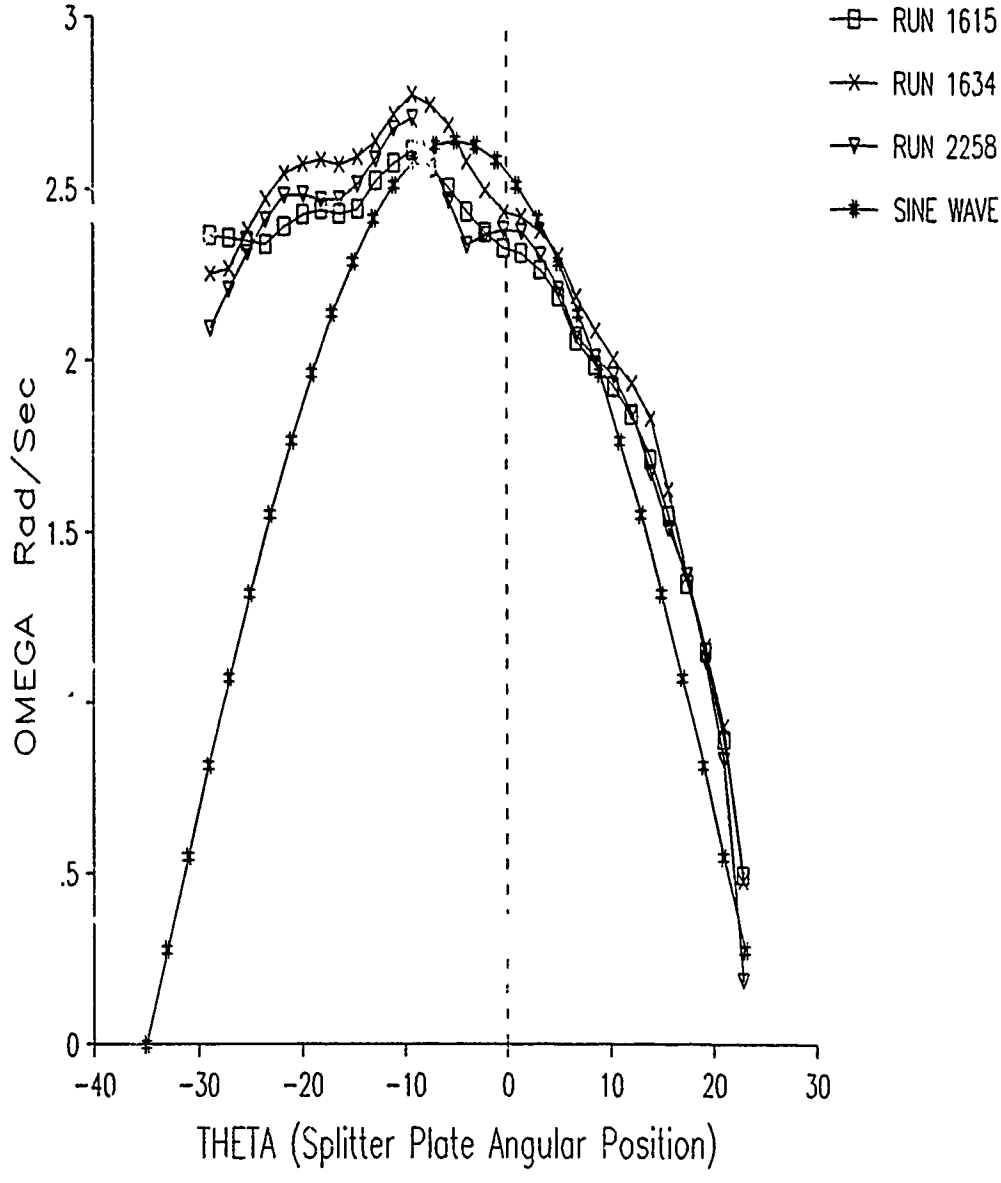

Fig. 4. Comparison of Measured Rotational Rates and True Sinusoidal Rate

Zero Data Files

Because of the inertial loads and moments produced simply by rotation of the mechanism, one cannot simply take "zero offset" data. In order to delineate between the zero loads and the aerodynamic loads, the "zero data" must be taken while the mechanism is rotating. To accomplish this, the mechanism was rotated at differing rates with tunnel air off and the resulting data was stored in a three-dimensional array which served as the "zero data" file. In order to extract a single channel zero reading, a double linear interpolation was required in the three-dimensional array depending on measured angular position and measured angular rotation rate. In this manner, the zero and inertial loads and moments were subtracted from the wind on overall data resulting in a measurement of the aerodynamic loads alone. For each new configuration in which the inertial loads would change, a new zero data file was generated.

RESULTS

Circulation Lag

As pointed out in Ref. 6, unsteady oscillations cause a delay or lag in the circulation around two-dimensional airfoils. This is also true of finite wings and is even more pronounced for rotation about a point not on the airfoil section. Figures 5 and 6 are summary plots of experimental data for a two wing configuration of equal span. (See Appendix 1, run numbers 0981, 1504 and 1517). The distance from the rotation point in the middle of the splitter plate to the leading edge of the forward and aft wings is eight inches (1.33 chord lengths). Data are taken during the oscillation as the plate traverses a negative to positive rotation angle. The steady-state data, run number 0981, indicates that the wing stalls at about 14 degrees for both the forward and aft wings. As the rotation rate is increased to a reduced frequency of .00155 as defined by Eq. 3 (corresponding to a rotation frequency of 0.192 Hz), the stall angle for both wings shifts to the right to a higher angle of attack. At higher reduced frequency rates of 0.00525 the stall angle shifts further to the right as expected. This circulation lag may be viewed as a shift in the angle for zero lift or it may be viewed as a change in normal force at alpha = 0.0. In either case, for the experiments documented in this report, the circulation lag is a nonlinear function of reduced frequency.

This circulation lag is dependent on the airfoil rotation rate; ie., reduced frequency, and the relative rotation axis location. As noted in Refs. 15 and 20, moving the pitching axis from the quarter chord location toward the trailing edge emulates the effects of an increased pitching rate. In the present experiments, moving the pivot axis off the airfoil trailing edge produces the same type

Run Numbers	Symbol	Wing Incidence Fwd	Wing Incidence Aft	Harmonic Freq. (Hz)	Wing Span Fwd	Wing Span Aft
0981	□	0	0	.00	18	18
1504	△	0	0	.20	18	18
1517	+	0	0	.60	18	18

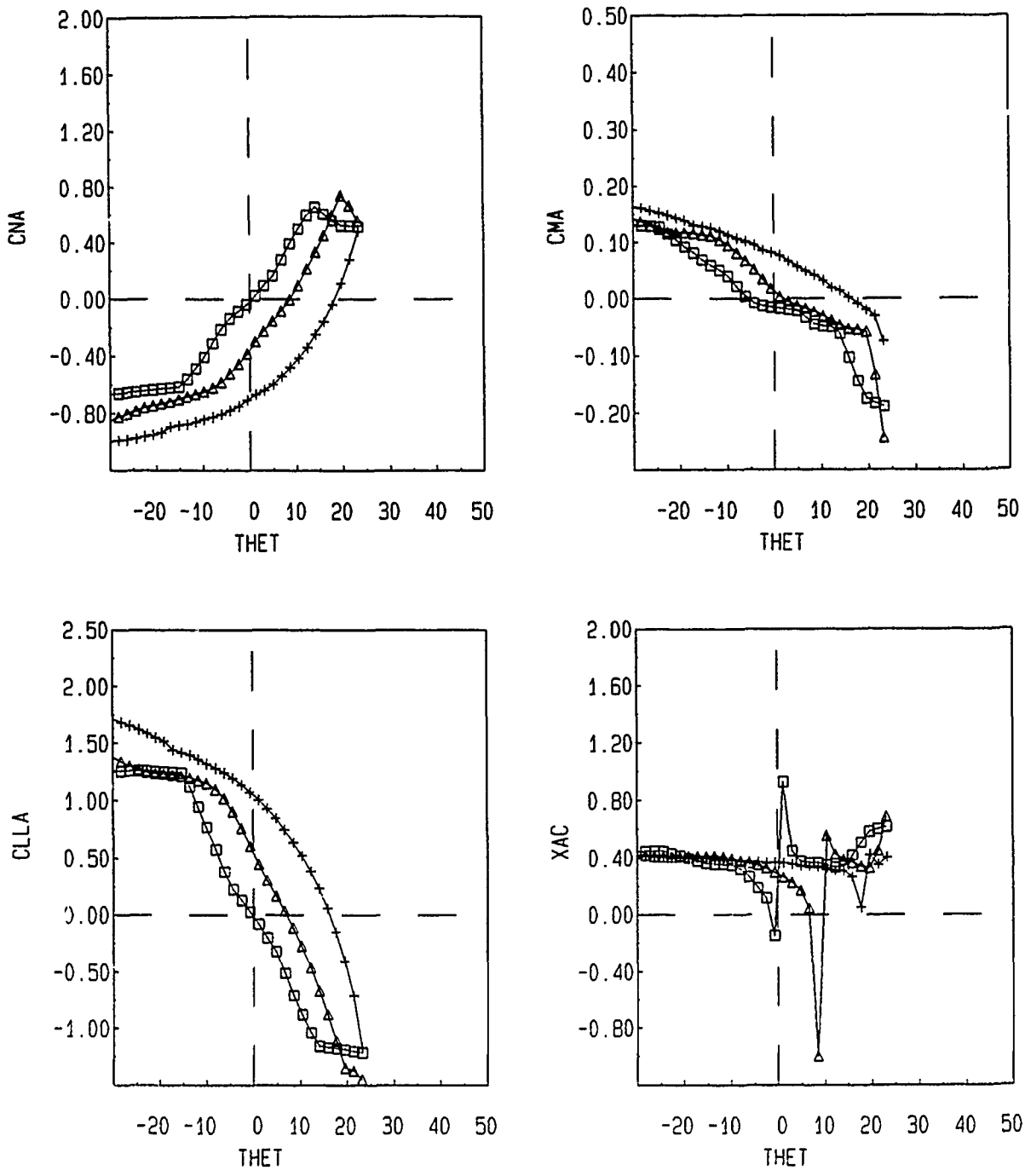

Fig. 5. Aft Wing Aerodynamic Coefficients versus Splitter Plate Angle of Attack (degrees)

Run Numbers	Symbol	Wing Incidence Fwd	Wing Incidence Aft	Harmonic Freq. (Hz)	Wing Span Fwd	Wing Span Aft
0981	□	0	0	.00	18	18
1504	△	0	0	.20	18	18
1517	+	0	0	.60	18	18

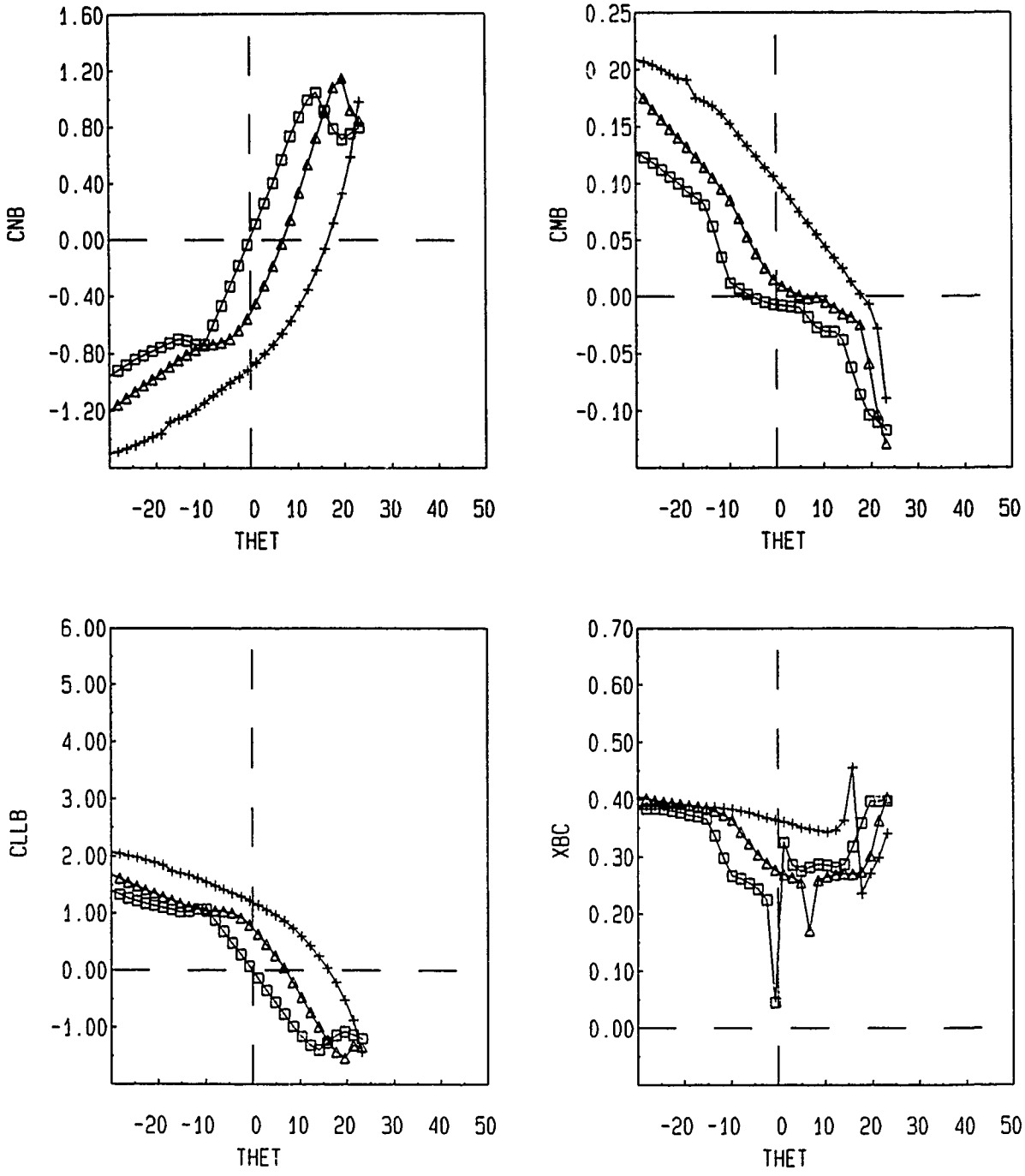

Fig. 6. Fwd Wing Aerodynamic Coefficients versus Splitter Plate Angle of Attack (degrees)

emulation as clearly seen in Fig. 6. The same can be said of moving the pivot axis forward toward the leading edge. In Fig. 5, note that the pivot axis is eight inches in front of the leading edge and the same lag in circulation occurs. In fact, when viewed from an angle of zero lift viewpoint, the results are essentially identical. These results and those of Refs. 15 and 20 clearly point out the need for including the pivot radius in the definition of reduced frequency as was previously suggested.

Changing the semispan of the forward wing, Figs. 7 and 8, or the aft wing, Figs. 9 and 10, does not alter the results. In fact, reducing the semispan 33% for the forward wing, as was done in Figs. 7-10, has little effect on the circulation lag associated with the aft wing. Further reduction in the semispan, however, may in fact change the circulation lag observations but it appears to be a two-dimensional phenomena dependent on the shed vorticity in the chordwise direction and essentially independent of the vortex trailing legs.

It may also be concluded that the circulation lag for an aft wing is not directly dependent on the downwash and, at best, is weakly influenced by the presence of an additional lifting surface. Figures 11 and 12 are results from isolated forward and aft wings and show no significant changes in the circulation lag from the two-wing case of Figs. 5 and 6. This is not to say, however, that the circulation lag and downwash are not in some way coupled as will be shown later.

It is clear from these results that the stall angle increases significantly with increases in rotation rate. However, the delineation between the "lift" stall and the "moment" stall is not apparent in the data as previously hypothesized. This is also apparent in the root chord bending moment data in Figs. 5-12 showing that the "bending moment" stall occurs at the same angle of attack as the "lift" and "pitching moment" stall. What these data do not show is the mechanism for the stall in an unsteady flow field.

Downwash

Downwash is a term loosely applied to the induced flow field surrounding a lifting surface. For many applications, this induced flow is treated as a "constant" and consequently can be related to an induced angle of attack. It is derived from the trailing legs of a vortex modeled lifting surface and mathematically is an inviscid phenomena governed by the three-dimensional Biot-Savart law. The trailing vortex filaments tend to "roll up" behind a finite wing and produce what is commonly termed a wing tip trailing vortex.

Only in certain idealized cases of a true elliptic spanwise load distribution will the trailing legs induce a uniform velocity along the quarter chord of an isolated finite wing. For a lifting surface placed in the wake of another lifting surface, the induced velocity; ie, induced angle of attack, or

Run Numbers	Symbol	Wing Incidence Fwd	Wing Incidence Aft	Harmonic Freq. (Hz)	Wing Span Fwd	Wing Span Aft
0980	□	0	0	.00	12	18
1933	△	0	0	.20	12	18
1946	+	0	0	.60	12	18

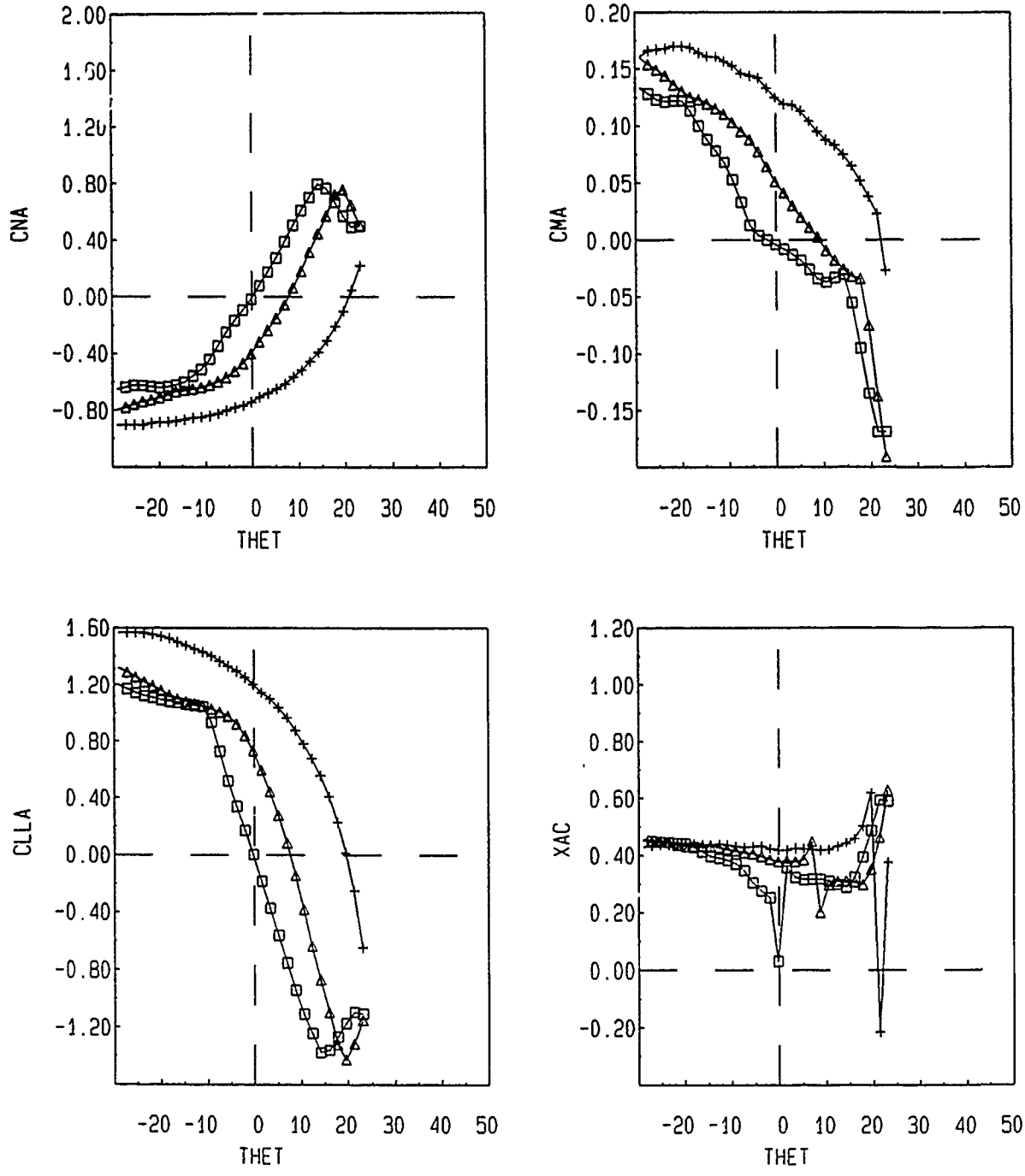

Fig. 7. Aft Wing Aerodynamic Coefficients versus Splitter Plate Angle of Attack (degrees)

Run Numbers	Symbol	Wing Incidence Fwd	Wing Incidence Aft	Harmonic Freq. (Hz)	Wing Span Fwd	Wing Span Aft
0980	□	0	0	.00	12	18
1933	△	0	0	.20	12	18
1946	+	0	0	.60	12	18

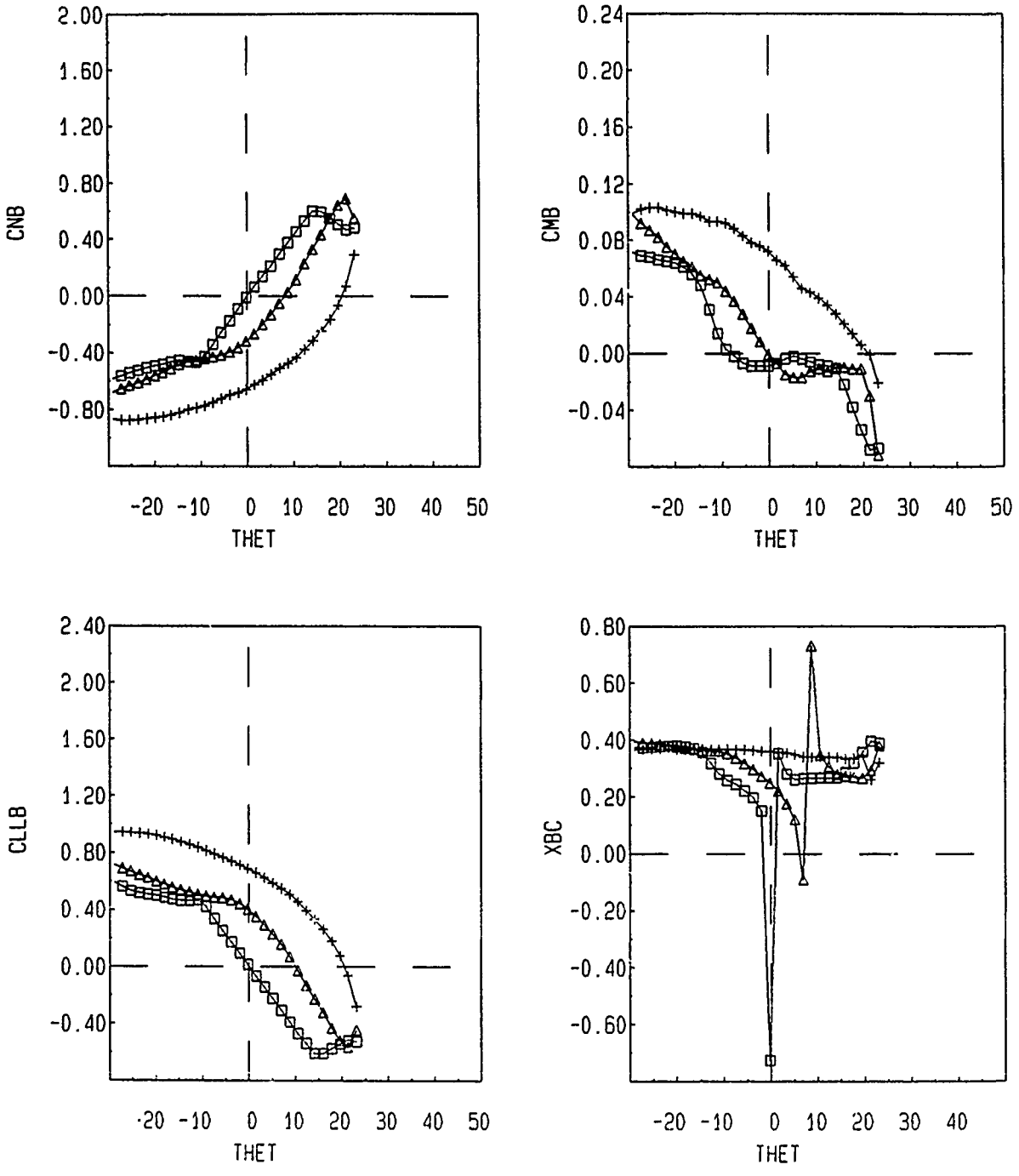

Fig. 8. Fwd Wing Aerodynamic Coefficients versus Splitter Plate Angle of Attack (degrees)

Run Numbers	Symbol	Wing Incidence Fwd	Aft	Harmonic Freq. (Hz)	Wing Span Fwd	Aft
0982	□	0	0	.00	18	12
2089	△	0	0	.20	18	12
2102	+	0	0	.60	18	12

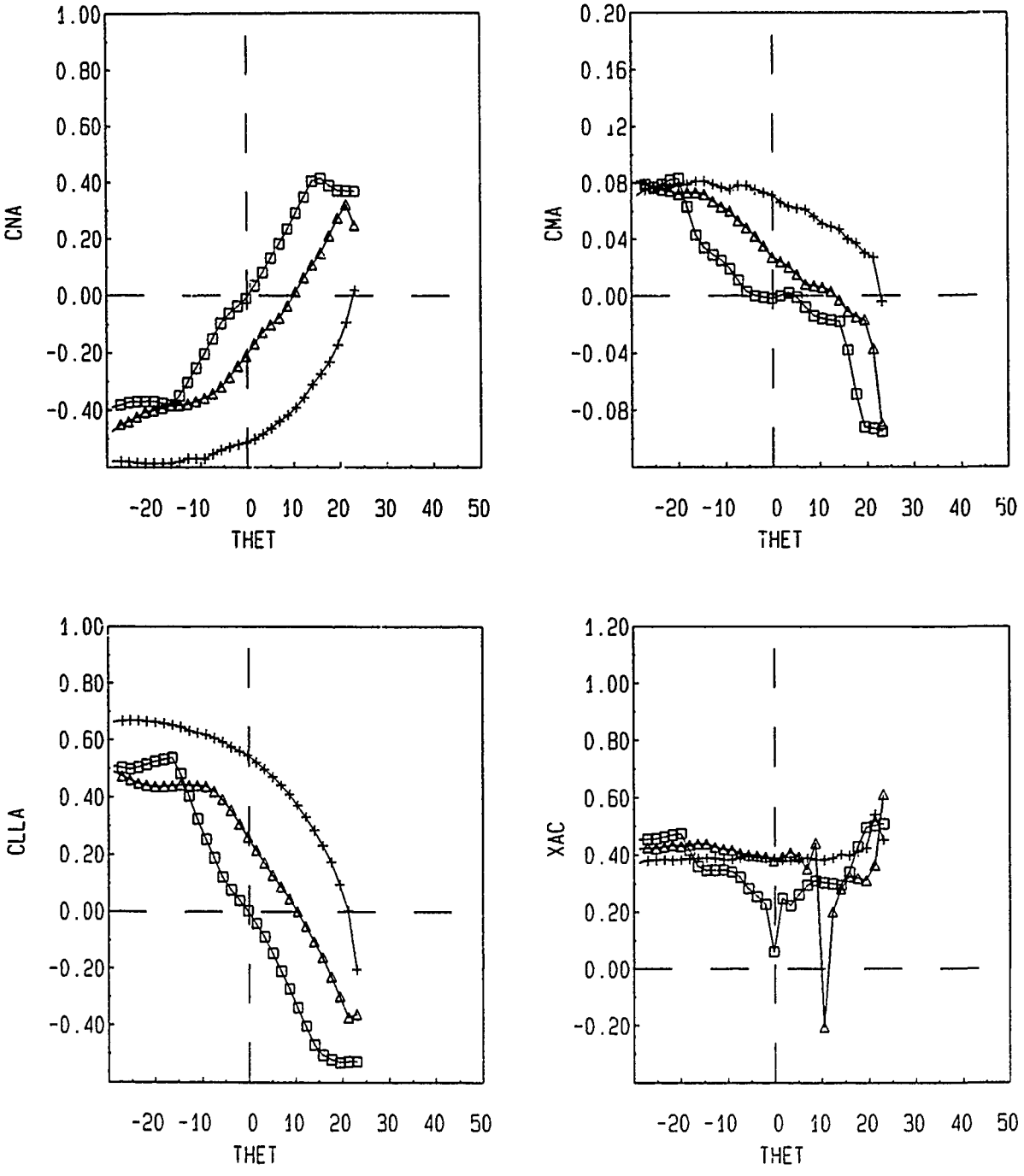

Fig. 9. Aft Wing Aerodynamic Coefficients versus Splitter Plate Angle of Attack (degrees)

Run Numbers	Symbol	Wing Incidence Fwd	Wing Incidence Aft	Harmonic Freq. (Hz)	Wing Span Fwd	Wing Span Aft
0982	□	0	0	.00	18	12
2089	△	0	0	.20	18	12
2102	+	0	0	.60	18	12

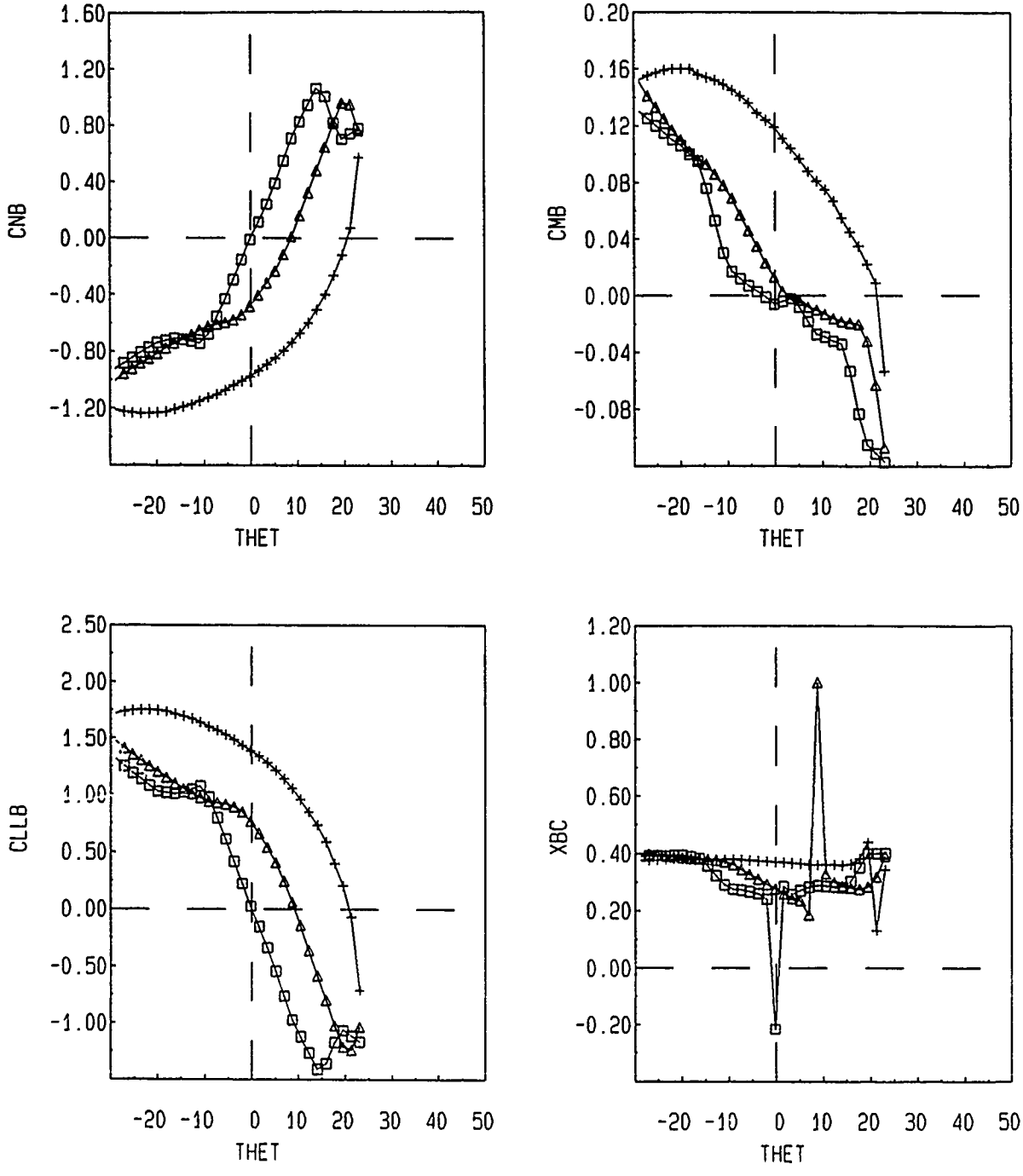

Fig. 10. Fwd Wing Aerodynamic Coefficients versus Splitter Plate Angle of Attack (degrees)

Run Numbers	Symbol	Wing Incidence Fwd	Wing Incidence Aft	Harmonic Freq. (Hz)	Wing Span Fwd	Wing Span Aft
0848	□	0	0	.00	0	18
1252	△	0	0	.20	0	18
1280	+	0	0	.60	0	18

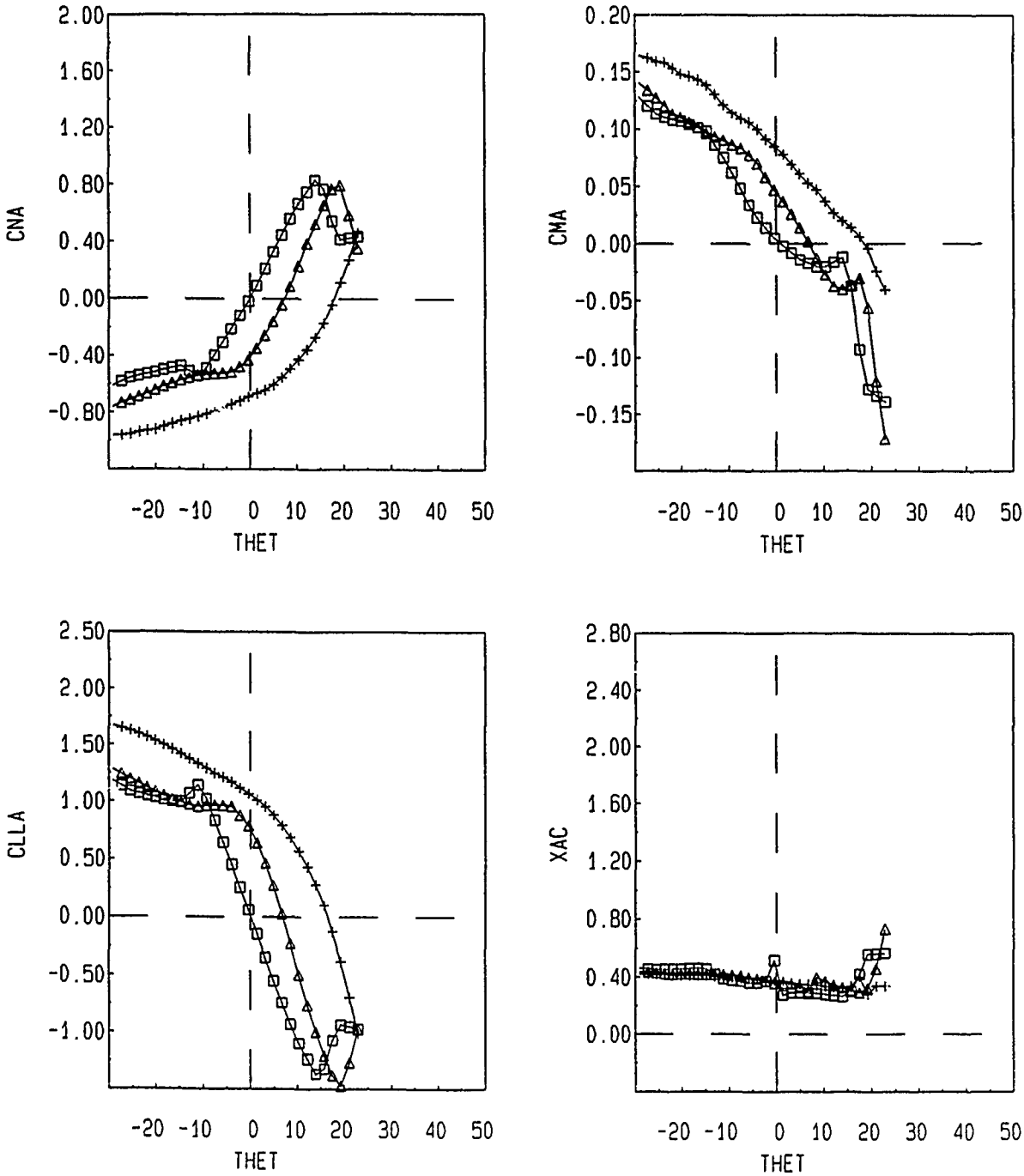

Fig. 11. Aft Wing Aerodynamic Coefficients versus Splitter Plate Angle of Attack (degrees)

Run Numbers	Symbol	Wing Incidence Fwd	Wing Incidence Aft	Harmonic Freq. (Hz)	Wing Span Fwd	Wing Span Aft
0849	□	0	0	.00	18	0
1000	△	0	0	.20	18	0
1084	+	0	0	.60	18	0

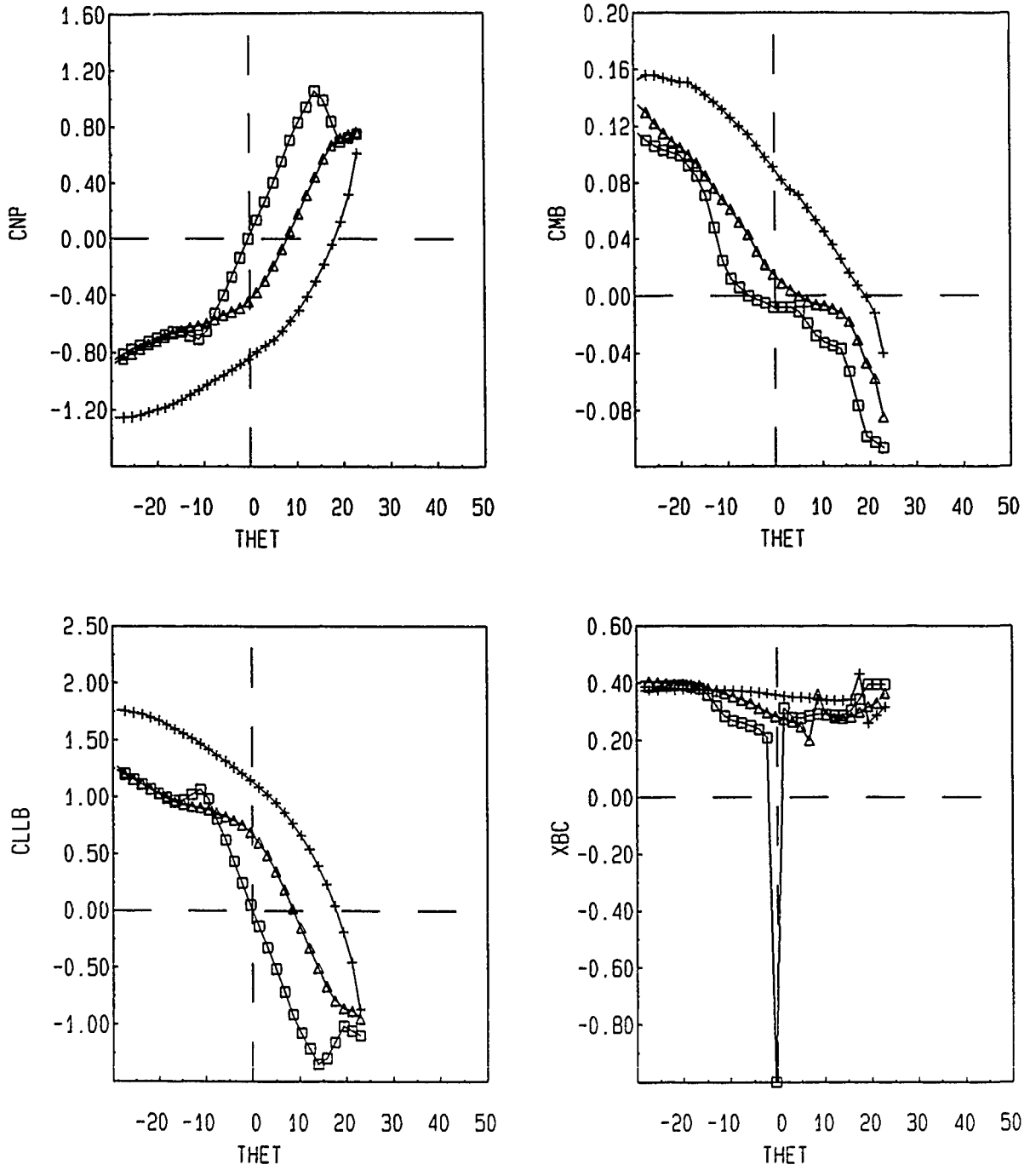

Fig. 12. Fwd Wing Aerodynamic Coefficients versus Splitter Plate Angle of Attack (degrees)

downwash, will never be uniform along the span of either wing. Consequently, one may view the flow field into which a lifting surface is placed as being non-uniform. For the unsteady case, the problem is even more complex since the "parent" flow field is also changing with time and spatial location. Though not well understood, the "downwash" can be measured in the steady or unsteady case.

If one considers a simplistic case of steady uniform flow with two lifting surfaces, then one expects to see a true "downwash" in the loading on the aft surface. As previously indicated, downwash may take the form of localized induced velocity measurements or globally as changes in the "normal" aerodynamic coefficient, although it is much easier to measure changes in the aerodynamic coefficients than to measure three-dimensional velocity components. When aerodynamic coefficients are to be used to describe downwash, two separate configurations must be utilized. First, coefficients for the wing of interest, say the aft wing, must be obtained with the "inducing" front wing not present. Secondly, the "forward" wing must be placed in the flow field and coefficients for the aft wing must be taken again. Results from these measurements for the aft wing are then subtracted yielding the difference as being indicative of the downwash. Of course, this approach does not yield localized flow field results, but does provide global changes in the lift, drag, side force, pitching moment, rolling moment, and yawing moment produced by the "front" wing downwash. For the present experiments, only the normal force, pitching moment, and root chord bending moment (rolling moment) were measured.

Figure 13 is a typical output for the case of two 18-inch wings as pictured schematically in Figs. 1-3. A positive downwash is defined to be a downward directed velocity component due to some inducing entity. In Fig. 13, a positive value for DCNA indicates that the isolated wing produced more normal force than the same wing in a two wing combination. That is, the presence of the forward wing reduced the normal force produced by the aft wing. For the steady-state case of Fig. 13, the loading on the aft wing behaves as expected at least for values of alpha between the stall angles (+/- 15 degrees); an upwash is measured for negative angles of attack and downwash for positive angles of attack. It appears as though the presence of the forward wing tends to reduce the pitching moment on the aft wing but in actuality the moment changes very little and this change can be attributed primarily to experimental error. This is perhaps more clearly seen from the data in Fig. 14. The center of pressure, XCPA, shifts slightly toward the nose, but again some of this shift can be attributed to experimental error.

When the whole system is oscillated at some global reduced frequency, as is the case in Figs. 15 and 16, several interesting observations can be made. First, the maximum value of the magnitude of the downwash changes very little as the reduced frequency is increased to 0.00155, Fig. 15, as defined by a global interpretation of Eq. (3). At higher reduced frequencies, Fig. 17,

Run Numbers	Symbol	Wing Incidence Fwd	Aft	Harmonic Freq. (Hz)	Wing Span Fwd	Aft
0848-0981	□	0	0	.00	18	18

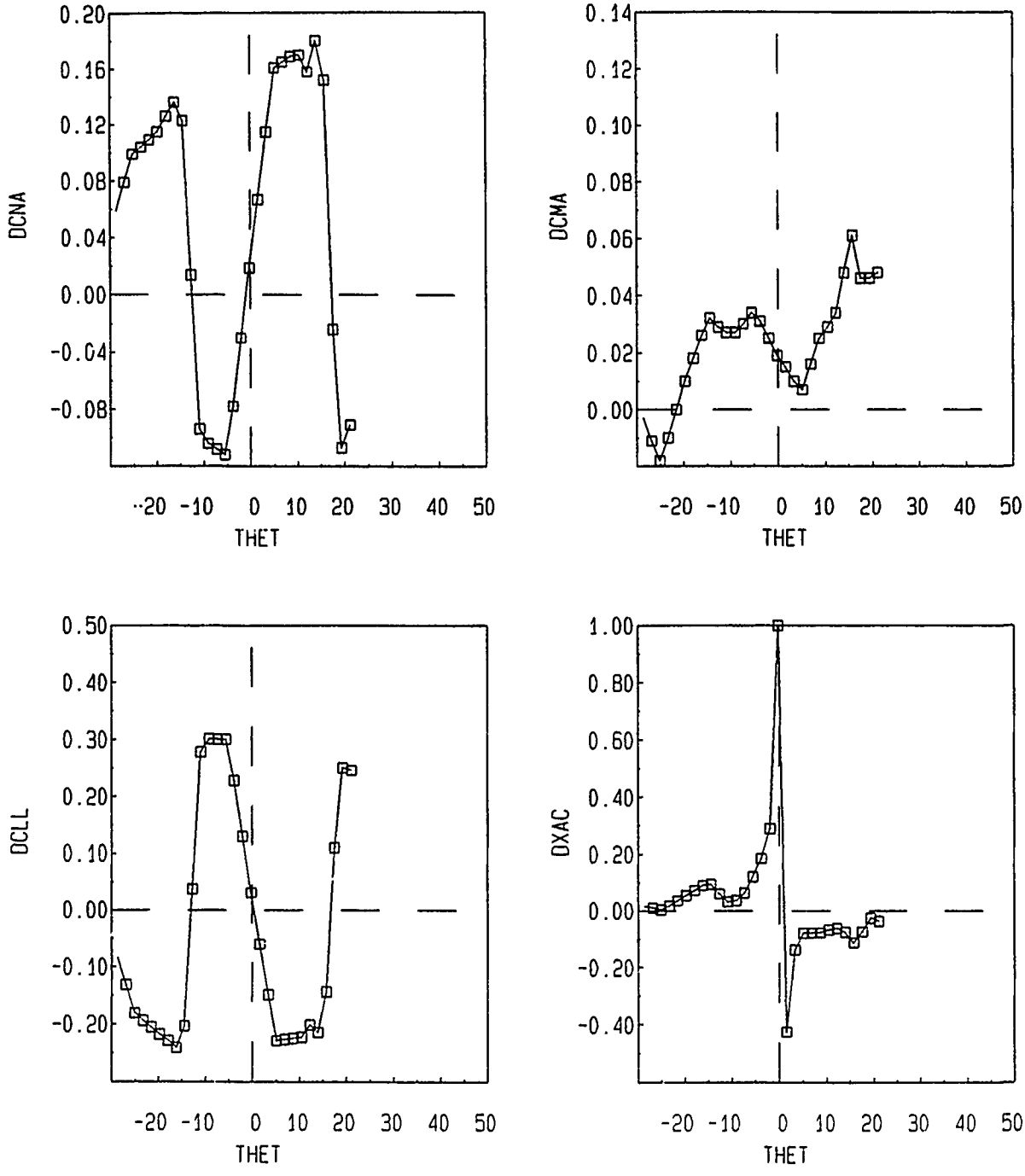

Fig. 13. Aft Wing Downwash Coefficients versus Splitter Plate Angle of Attack (degrees)

Run Numbers	Symbol	Wing Incidence Fwd	Wing Incidence Aft	Harmonic Freq. (Hz)	Wing Span Fwd	Wing Span Aft
0848	□	0	0	.00	00	18
0981	△	0	0	.00	18	18

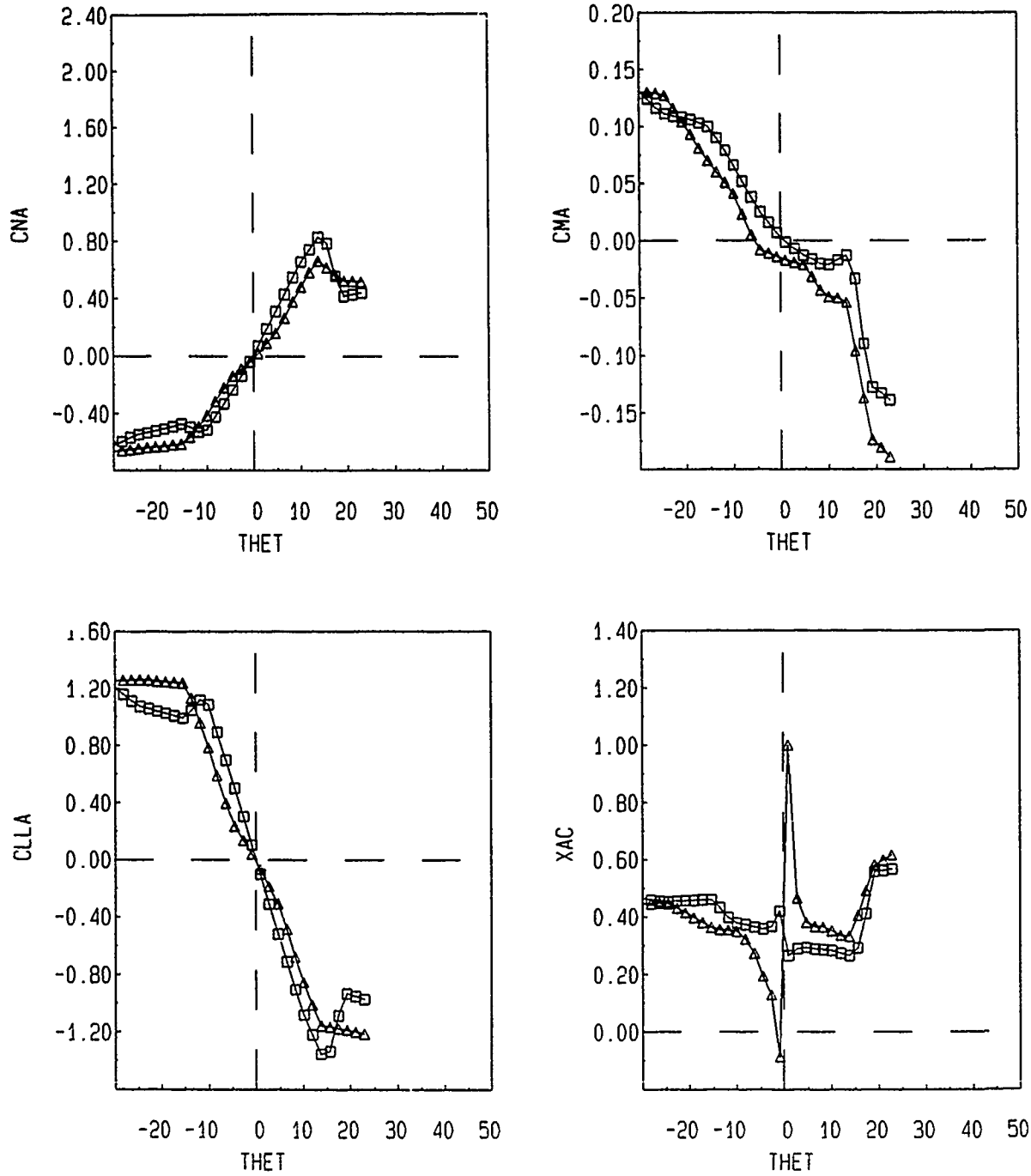

Fig. 14. Aft Wing Aerodynamic Coefficients versus Splitter Plate Angle of Attack (degrees)

Run Numbers	Symbol	Wing Incidence Fwd	Aft	Harmonic Freq. (Hz)	Wing Span Fwd	Aft
1252-1504	□	00	0	.20	18	18
1252-1506	△	10	0	.20	18	18
1252-1509	+	-10	0	.20	18	18

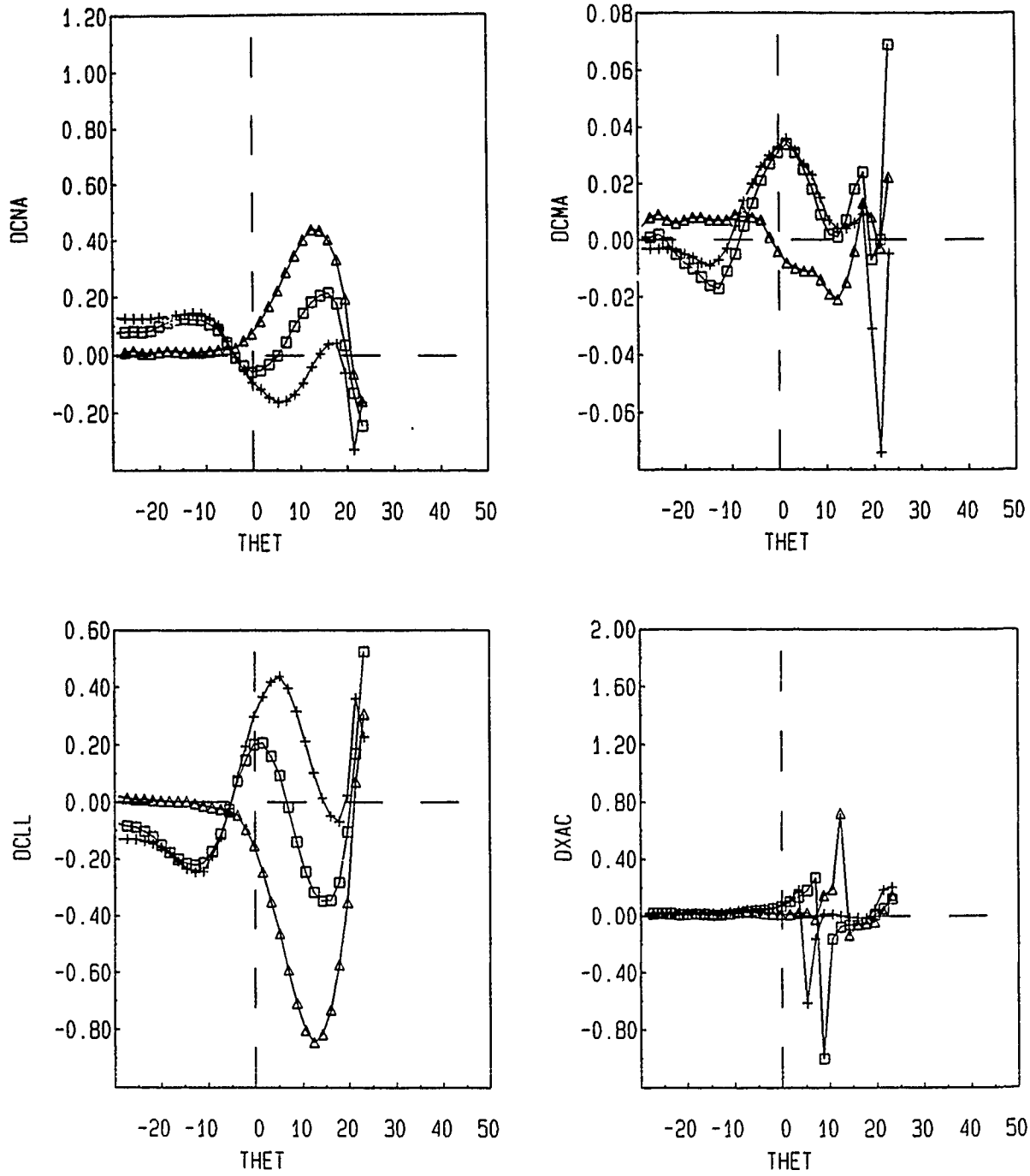

Fig. 15. Aft Wing Downwash Coefficients versus Splitter Plate Angle of Attack (degrees)

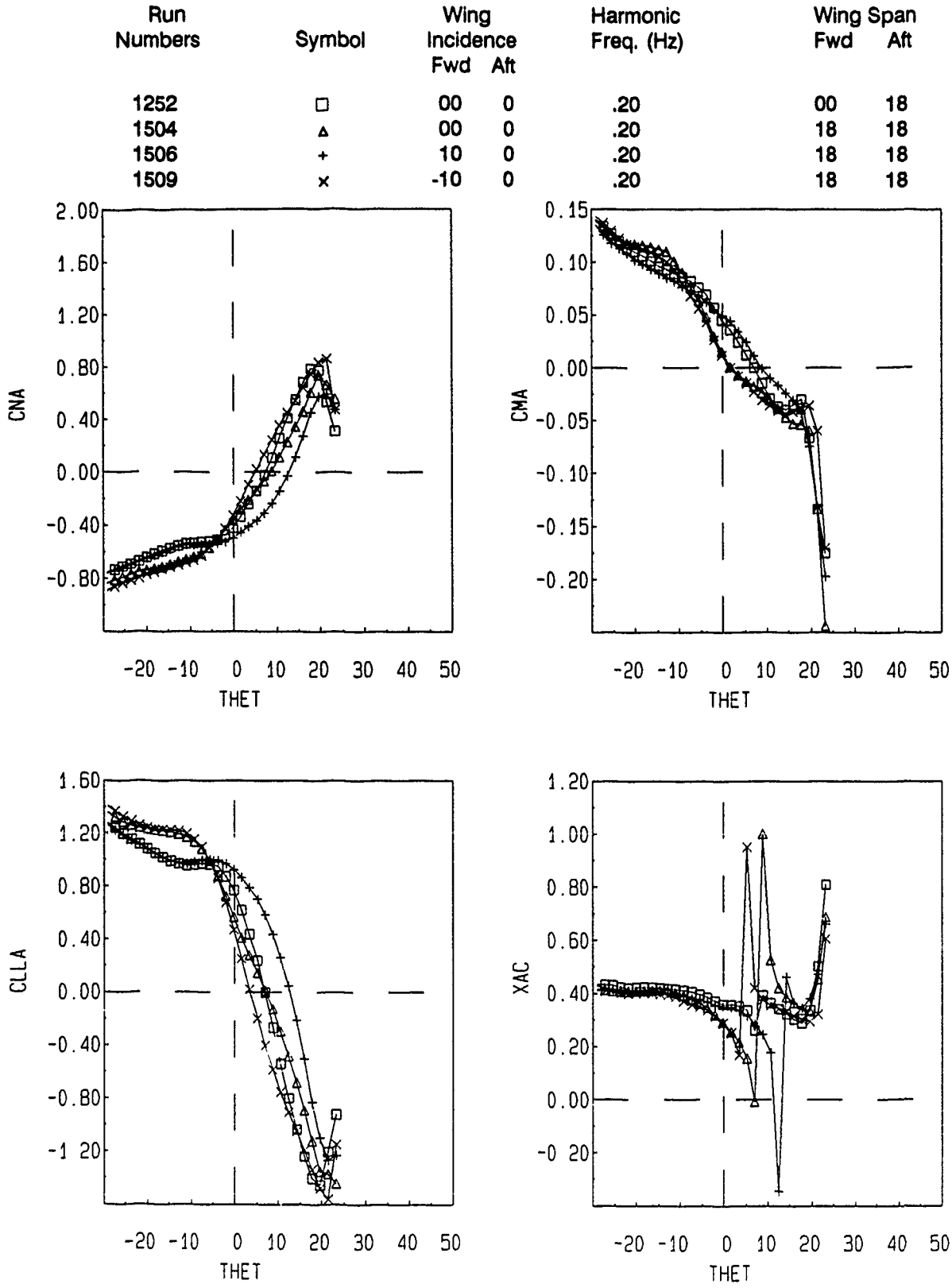

Fig. 16. Aft Wing Aerodynamic Coefficients versus Splitter Plate Angle of Attack (degrees)

Run Numbers	Symbol	Wing Incidence Fwd	Aft	Harmonic Freq. (Hz)	Wing Span Fwd	Aft
1280-1517	□	00	0	.60	18	18
1280-1519	△	10	0	.60	18	18
1280-1522	+	-10	0	.60	18	18

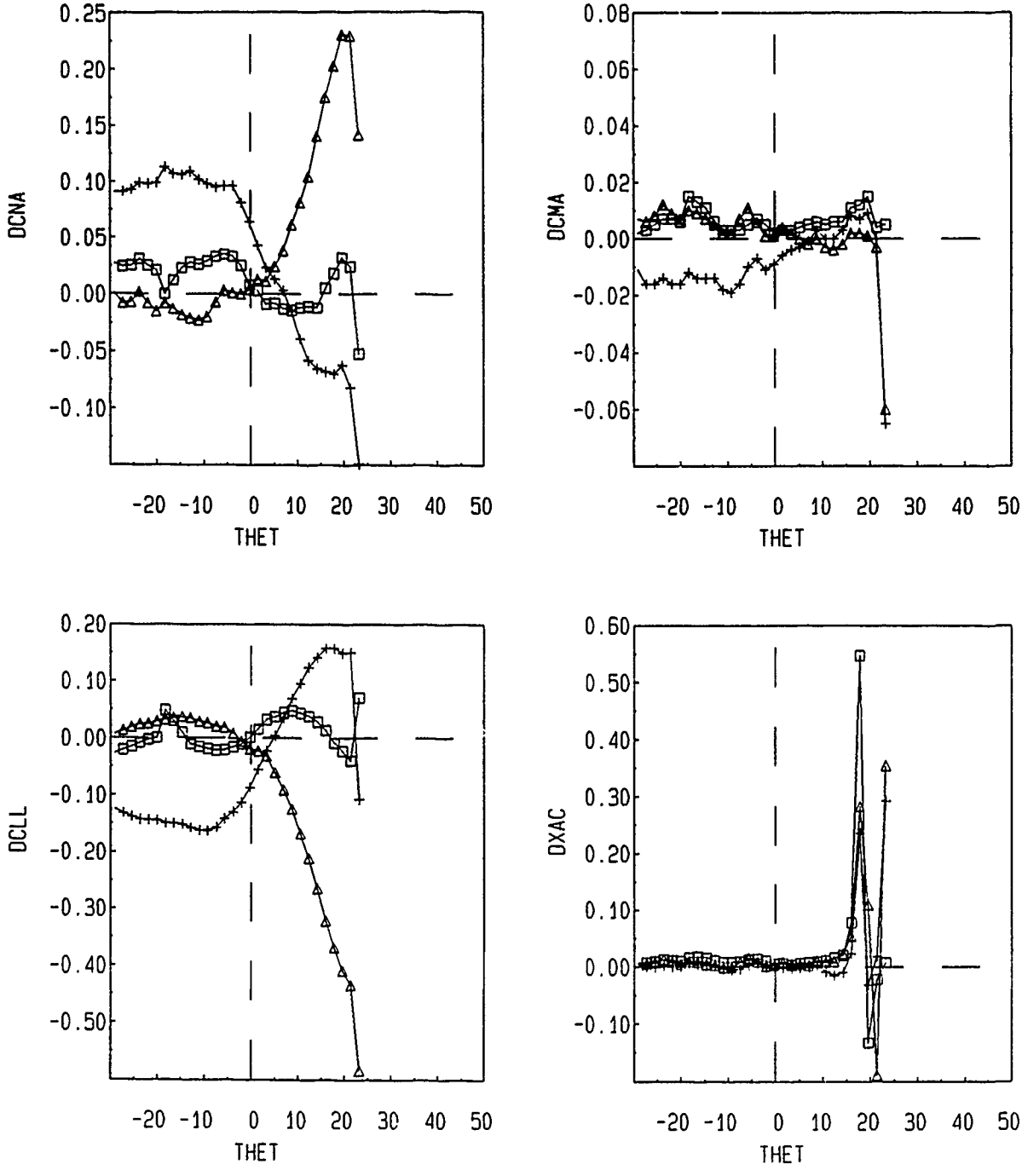

Fig. 17. Aft Wing Downwash Coefficients versus Splitter Plate Angle of Attack (degrees)

measured values of downwash drops essentially to zero. This can perhaps be explained by noting that at very high reduced frequencies, the downwash is probably masked by changes in loading due to circulation lag even though the normal force coefficients continue to increase as previously noted.

Secondly, even though the magnitude of the downwash changes very little, the downwash curve is shifted in angle of attack to the right. That is, maximum upwash does not occur at the negative stall angle, but for this particular case occurs at near zero angle of attack. The shift in the downwash curve is essentially the same as the shift in alpha due to circulation lag on the aft wing section. That is, the shift in the downwash curve is due to circulation lag of the aft wing coupled with the loading on the forward wing. There is no discernable lag due to the flow speed or angular rotation speed.

If one now changes the incidence of the forward wing, Figs. 15 and 16, the magnitude of the downwash is altered accordingly, indicating that downwash is directly dependent on the loading of the forward wing even though this loading is shifted in angle of attack. The important observation here is that the magnitude of the shift is dependent on the incidence of the forward wing. If the incidence is positive (positive angle of attack), the magnitude of the downwash increases significantly and "unloads" the aft wing accordingly causing it to produce less lift, but it also shifts the peak value to smaller positive angles of attack. If the incidence is negative (negative angle of attack), the shift in the downwash curve is to the right, because of the circulation lag, so that the "downwash" becomes upwash on the aft wing causing it to produce more lift.

What does this really mean from a practical standpoint? Consider an idealized canard-controlled agile fighter which is to perform a rapid translation to a higher altitude. Normally one would move the canard to a positive incidence angle in order to pitch the aircraft up to a higher positive angle of attack. If the rotation rate of the entire aircraft is moderately rapid, the increased normal force on the canard will produce a large downwash on the aft main wing and reduce its effectiveness in producing lift. However, if during the pitch up maneuver the canard is lowered to a negative incidence, upwash is produced on the aft main wing and causes significantly more lift to be developed and consequently a rapid altitude change.

This concept is "somewhat" related to the roll reversal problem encountered in some missile designs. Consider the case of a cruciform missile with canards for pitch, yaw, and roll control and large main wings for producing lift and side force. A simple roll maneuver to the left requires that the right canard rotate up and the left canard rotate down producing a moment intended to roll the airframe to the left. However, a positive normal force on the right canard produces downwash on the right wing and a negative normal force on the left canard produces upwash on the left wing. If the downwash on the right wing and upwash on the left wing surface is large enough, the

resulting moment may be sufficient to roll the airframe to the right opposing the left roll being produced by the canard deflection, a classic case of roll reversal. It may be possible that this concept, coupled with the unsteady flow circulation lag can be used to an advantage. Practical implementation of this phenomena is still perhaps in the future.

Center of Pressure

In all the present experimental measurements of downwash, Figs. 13, 15, and 17 indicate that there is little change in the aft wing center of pressure. That is, the downwash produced on the aft wing does not change the aft wing center of pressure very much. Rolling moment and aft wing pitching follow basic trends of the aft wing normal force. The spanwise center of pressure usually ranged between the 55 to 70 percent span point.

Semispan Effects

Since downwash is directly dependent on the loads being produced, changing the forward wing semispan, as is done in Figs. 18-21, of course changes the magnitude of the downwash, but does not alter the final conclusions. That is, the steady-state data in Figs. 18 and 19 follow the same trends as previous steady-state data but with a reduction in magnitude. For the unsteady case, Figs. 20 and 21, the general trends remain the same so that a negative incidence angle for the forward canard produces upwash on the aft wing giving rise to an increase in the normal force capability of the aft wing at positive angles of attack (see Fig. 21). The reason for the net upwash on the aft wing is basically tied to the lag in the circulation around the forward wing coupled with the lag in circulation around the aft wing. The mechanism for the coupling between the forward wing downwash/upwash, the forward wing circulation lag, and the aft wing circulation lag is not fully understood. It appears, however, that any delay in the "influence" of the loading on the forward wing and the loading on the aft wing is on the order of the time required for the flow to traverse the distance between the two wings which, for these cases, is very short. Figure 22 is a plot of the normal force coefficient for the front wing for an 18-inch span (top) and for a 12-inch span (bottom). Incidence angles are noted and the circulation lag for each is clearly apparent. Note that for both these cases, at large angles of attack, the normal force becomes positive even for negative incidence angles, but the downwash on the aft wing is still "upwash" (see Figs. 15 and 21) producing an increased normal force on the aft wing.

Run Numbers	Symbol	Wing Incidence Fwd	Wing Incidence Aft	Harmonic Freq. (Hz)	Wing Span Fwd	Wing Span Aft
0848	□	0	0	.00	00	18
0980	△	0	0	.00	12	18

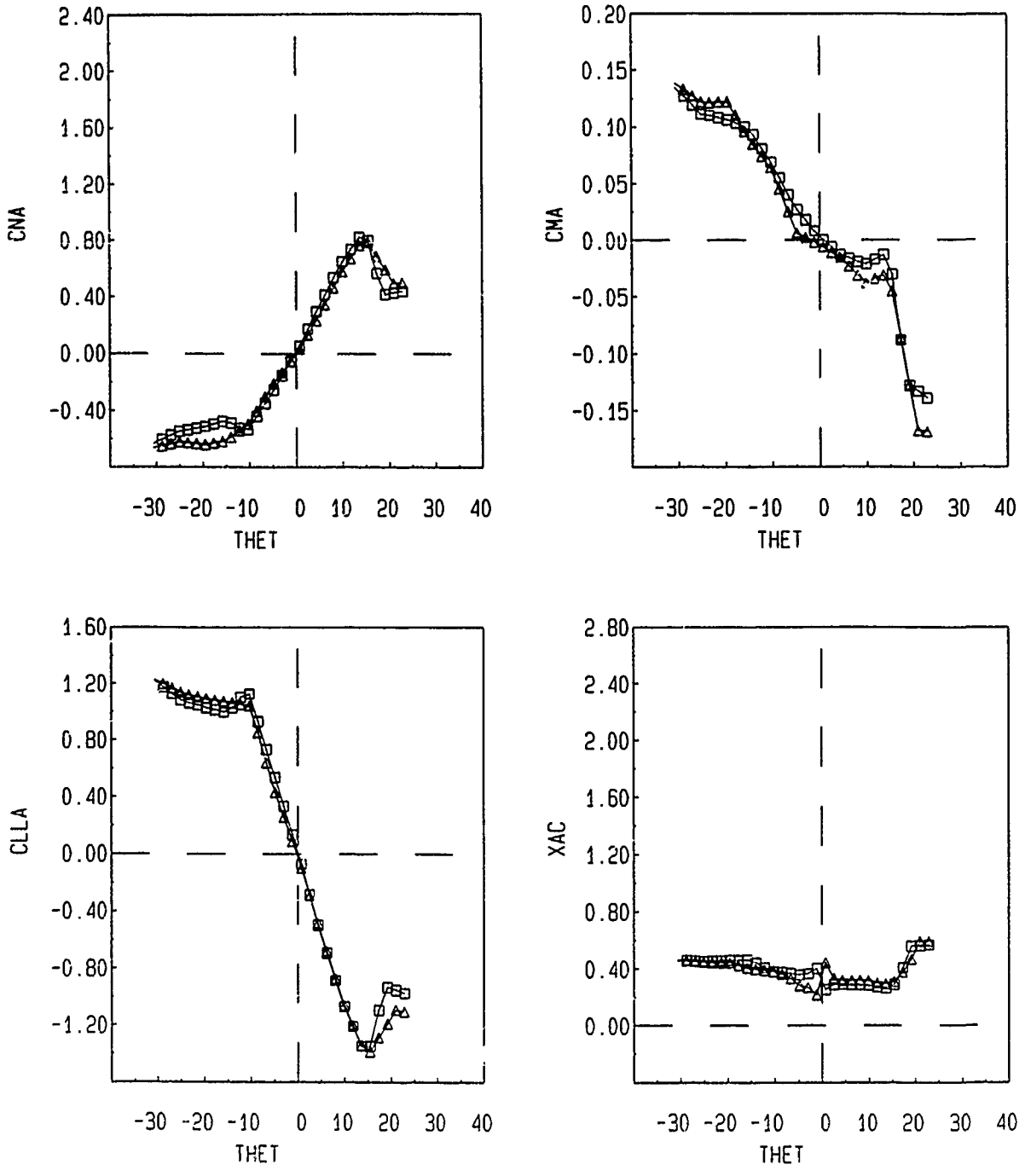

Fig. 18. Aft Wing Aerodynamic Coefficients versus Splitter Plate Angle of Attack (degrees)

Run Numbers	Symbol	Wing Incidence Fwd	Wing Incidence Aft	Harmonic Freq. (Hz)	Wing Span Fwd	Wing Span Aft
0848-0980	□	0	0	.00	12	18

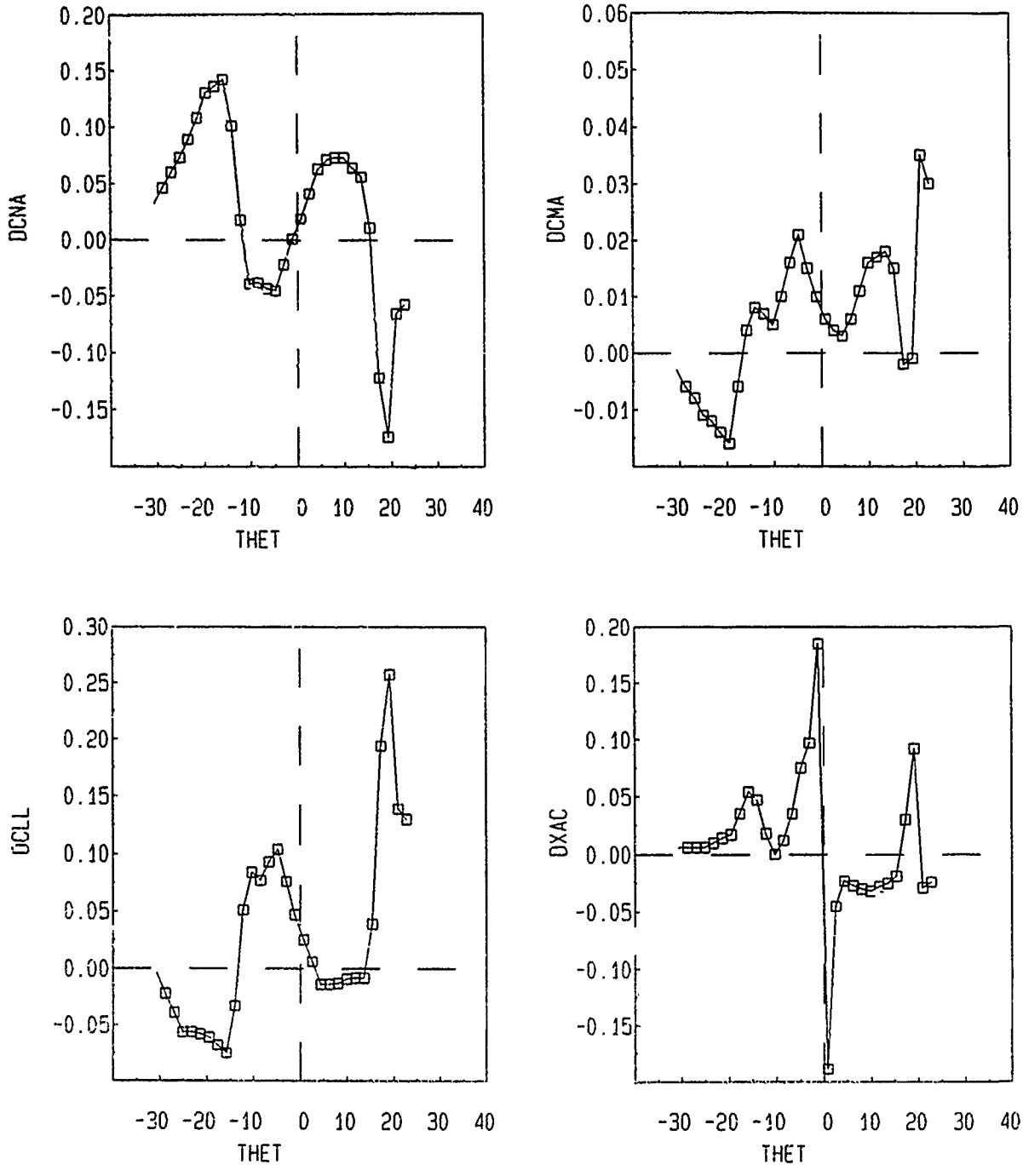

Fig. 19. Aft Wing Downwash Coefficients versus Splitter Plate Angle of Attack (degrees)

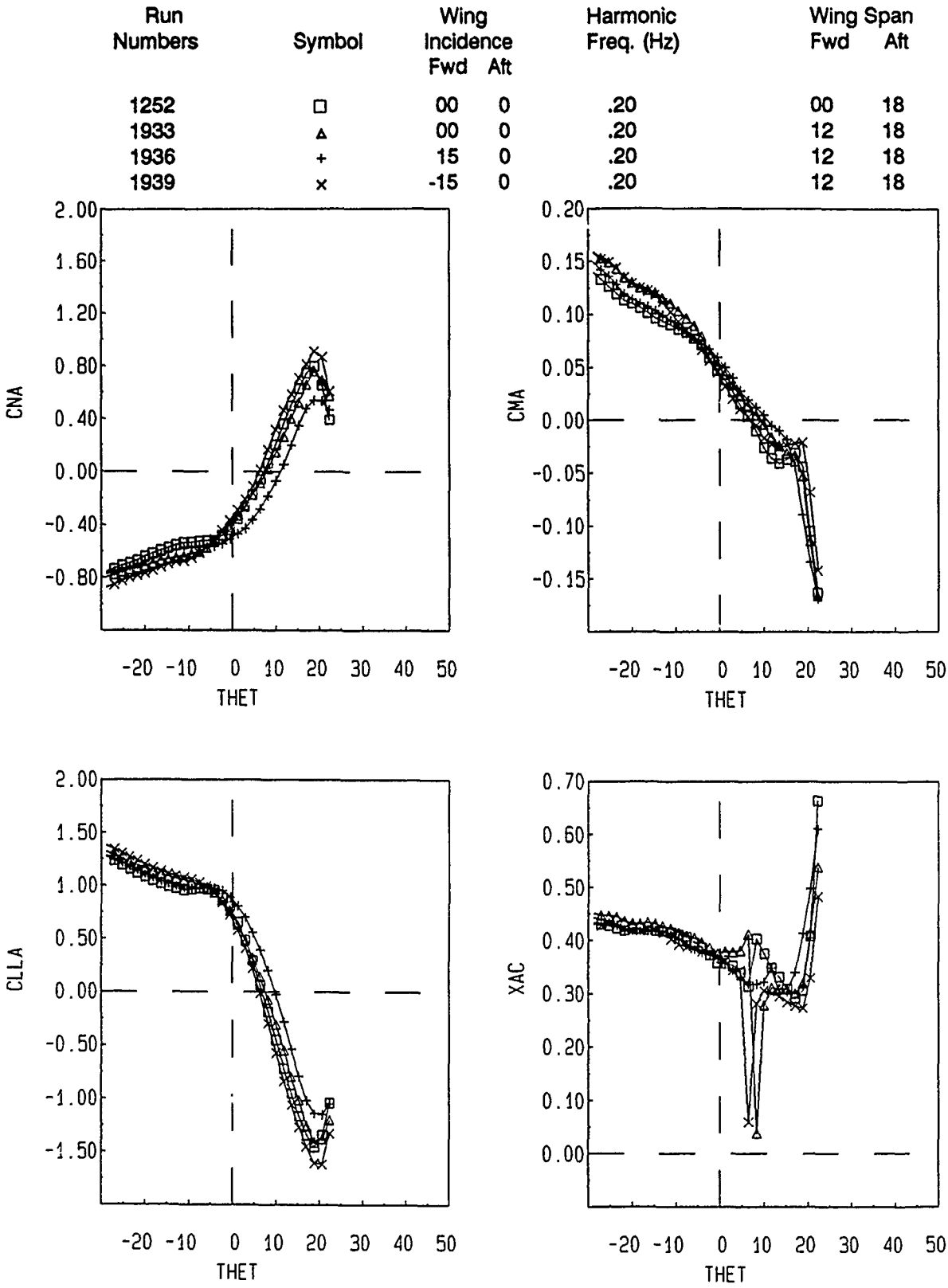

Fig. 20. Aft Wing Aerodynamic Coefficients versus Splitter Plate Angle of Attack (degrees)

Run Numbers	Symbol	Wing Incidence Fwd	Aft	Harmonic Freq. (Hz)	Wing Span Fwd	Aft
1252-1933	□	00	0	.20	12	18
1252-1936	△	15	0	.20	12	18
1252-1939	+	-15	0	.20	12	18

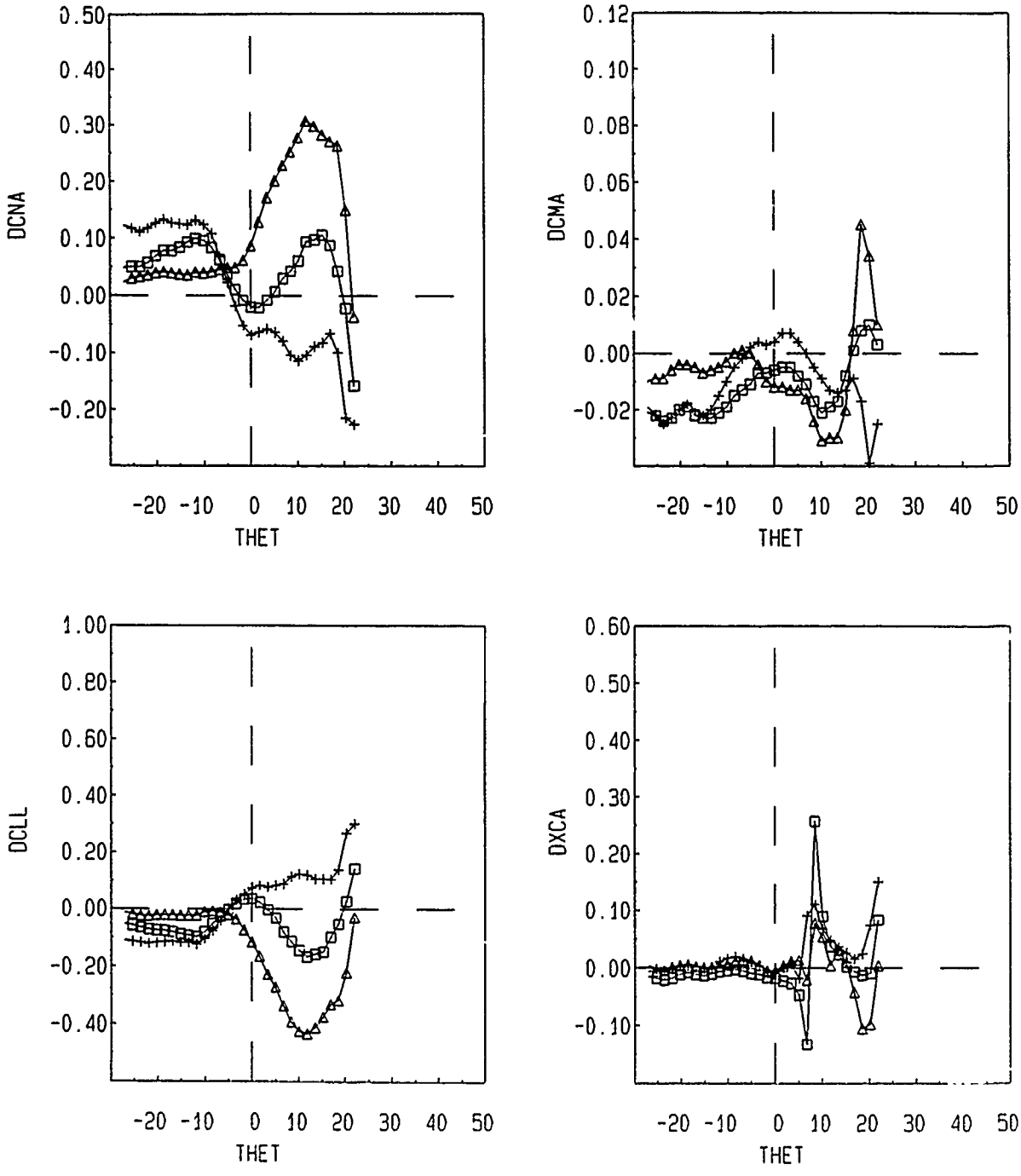

Fig. 21. Aft Wing Downwash Coefficients versus Splitter Plate Angle of Attack (degrees)

Run Numbers Top	Run Numbers Bot	Symbol	Aft Wing Incidence Top	Aft Wing Incidence Bot	Harmonic Freq. (Hz)	Wing Span Top Fwd	Wing Span Top Aft	Wing Span Bottom Fwd	Wing Span Bottom Aft
1504	1933	□	00	00	.20	18	18	18	12
1506	1936	△	15	15	.20	18	18	18	12
1509	1939	+	-15	-15	.20	18	18	18	12

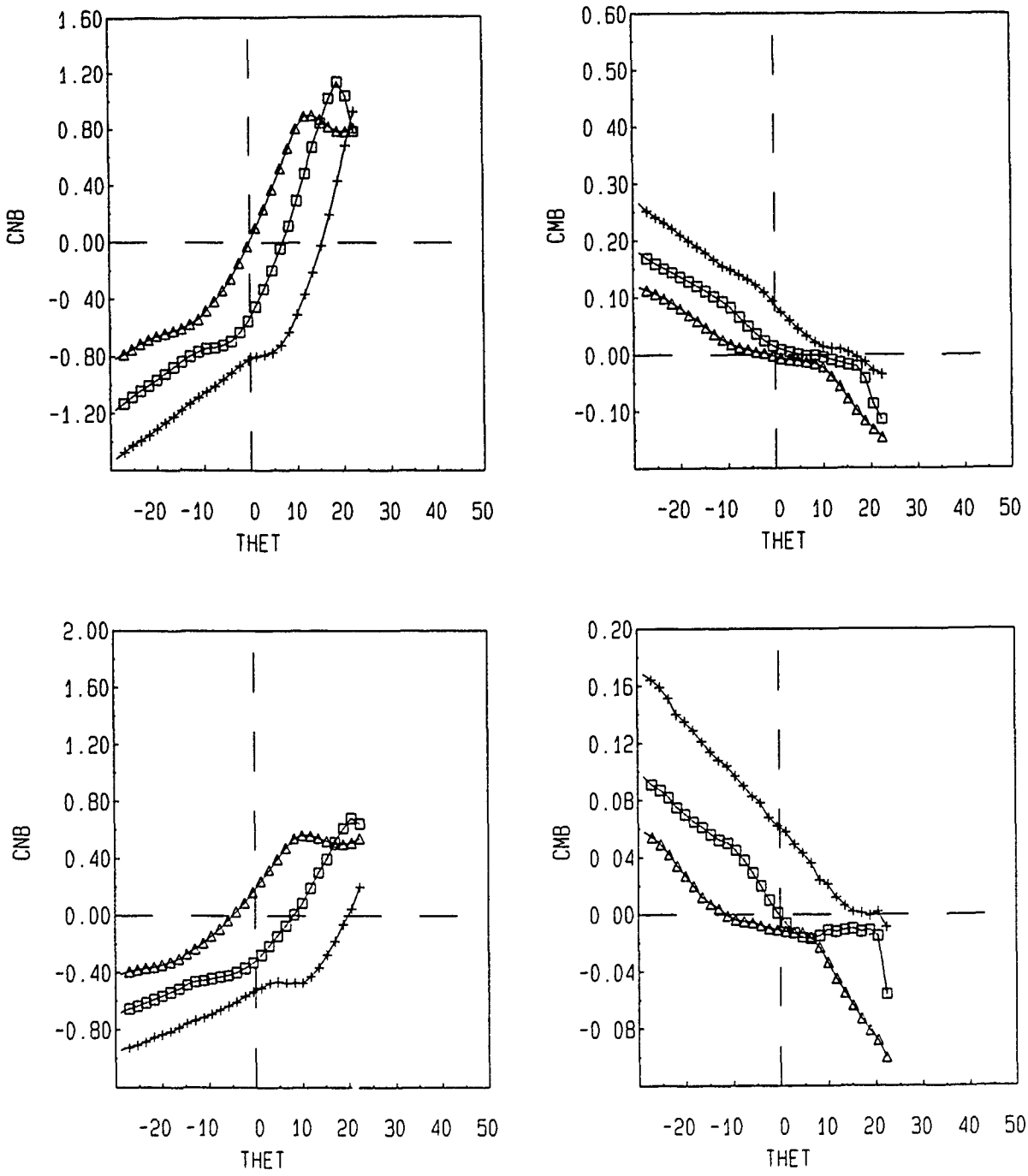

Fig. 22. Fwd Wing Aerodynamic Coefficients versus Splitter Plate Angle of Attack (degrees)

Wing Separation Effects

Before the wind tunnel tests were run it was not clear what effect, if any, that a vertical separation between the canard and main wing would have on the circulation lag and/or the downwash. To determine this dependency in a qualitative manner, several runs were made with various separation distances, both positive and negative, and an abbreviated summary of the results are presented in Fig. 23. All runs are not presented, but from these data it appears that a canard above the main wing would be preferable. From Fig. 23, it is shown that if it is desired to produce upwash during a pitch up maneuver, then clearly the canard should be placed above the main wing. For the configuration tested, placing the canard below the main wing produces essentially no upwash or significant downwash, thereby decreasing the aft wing's ability to produce lift.

Dihedral effects

A similar study, as for wing separation effects, was done for dihedral effects. For the 10 degree aft wing dihedral depicted in Fig. 24, the influence of forward wing dihedral to produce upwash is marginal at best. For these data, there is no strong dihedral dependency and is probably an order of magnitude less than the wing separation effects. There appears to be no coupling between dihedral of either wing and the circulation lag and/or induced downwash.

CONCLUSIONS

The results of the present study have led to several conclusions, some of which confirm other experimental and theoretical results and others which provide new insights into the complex problem associated with unsteady flows. From the present test results the following conclusions are made.

(1) Circulation lag associated with oscillating wings is an important fundamental property of the flow field. It is essentially independent of external induced downwash flow fields but is dependent on the location of the pivot point for the wing or airfoil section, the starting and ending angle of the oscillation, and the angle of attack history of the lifting surface.

(2) Reduced frequency definitions in the technical literature are somewhat inconsistent. The recommendation that the definition of the nondimensional reduced frequency be the ratio of the wing/airfoil leading edge rotational velocity to the free stream velocity appears to satisfy the requirements for similarity matching.

Run Numbers	Symbol	Wing Separation	Harmonic Freq. (Hz)	Wing Span Fwd	Aft
1252-1751	□	3.171"	.20	18	18
1252-1881	△	-3.171"	.20	18	18

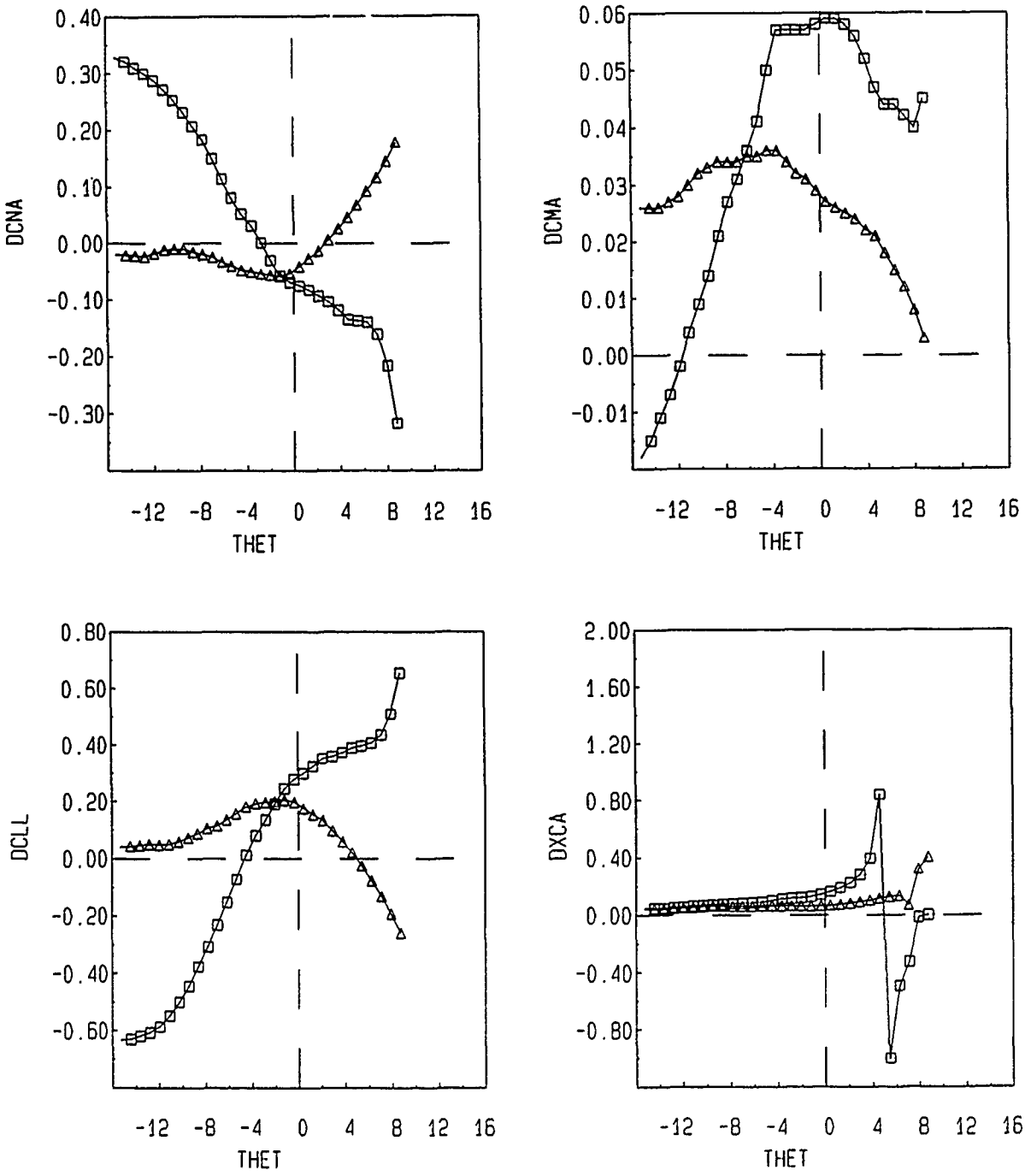

Fig. 23. Aft Wing Downwash Coefficients versus Splitter Plate Angle of Attack (degrees)

Run Numbers	Symbol	Wing Dihedral Fwd	Wing Dihedral Aft	Harmonic Freq. (Hz)	Wing Span Fwd	Wing Span Aft
0864-0877	□	-10	10	.00	18	18
1266-1595	△	-10	10	.20	18	18

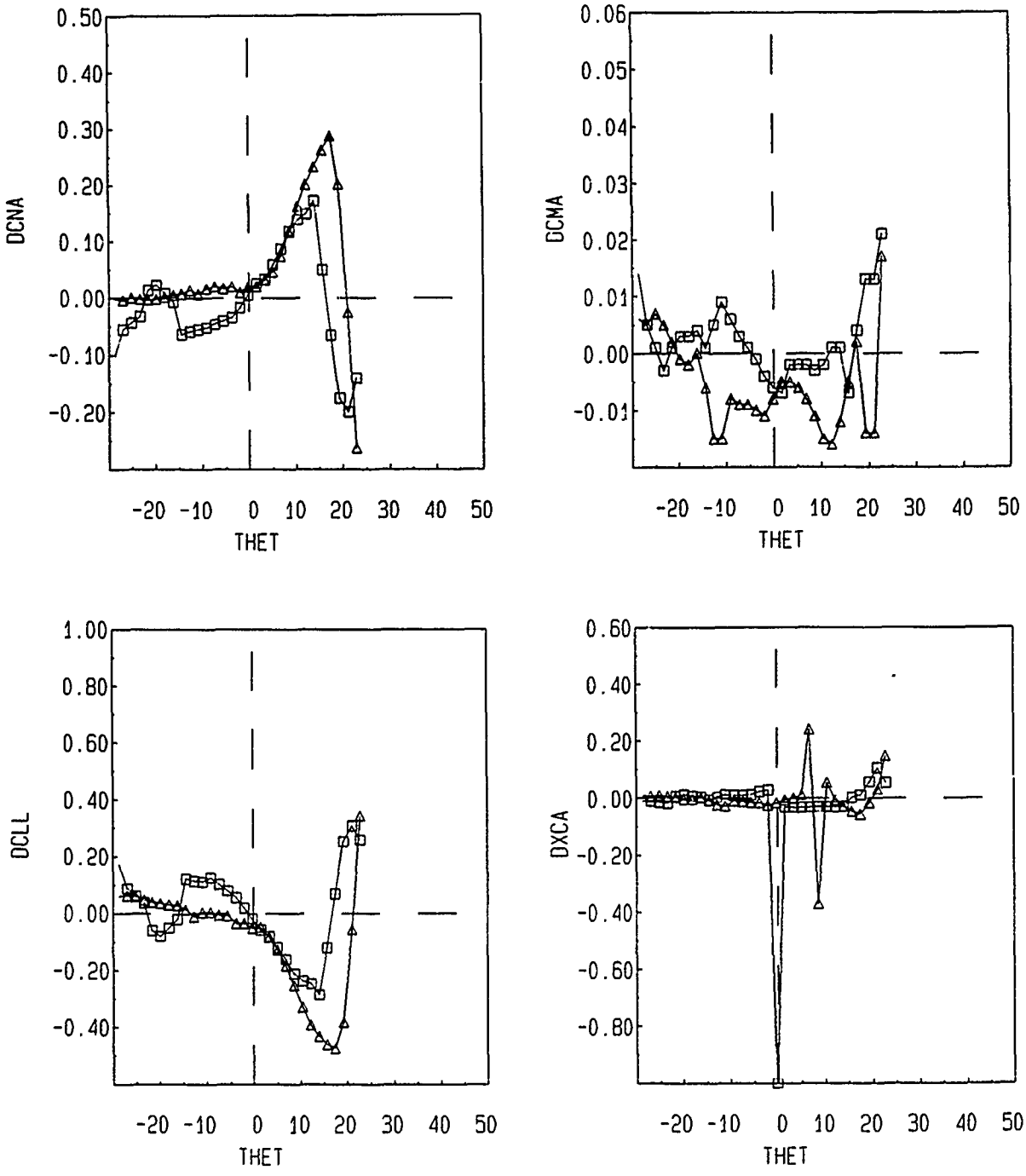

Fig. 24. Aft Wing Downwash Coefficients versus Splitter Plate Angle of Attack (degrees)

(3) Downwash from a forward wing on an aft lifting surface can make a significant contribution to the lifting properties of the aft wing. The magnitude of these downwash forces are dependent on the forward wing normal force magnitudes and may enhance or degrade the potential of an aft wing to produce lift.

(4) It is clear, in an oscillating two-wing configuration, that both the forward wing and the aft wing have an associated circulation lag. The downwash induced in this case, however, is not synchronized with the circulation lag for the downwash producing front wing but the shift in the downwash curve is more or less synchronized with the circulation lag associated with the aft wing. Consequently, a forward wing producing positive lift can produce upwash on an aft located wing increasing its potential to produce lift.

(5) As a general rule, for an enhanced maneuverable aircraft which is canard controlled, the forward canard should be placed above the main wing lifting surface.

(6) There is no strong dihedral dependency and no strong coupling between dihedral of either wing and the circulation lag and/or induced downwash.

RECOMMENDATIONS FOR FURTHER STUDY

(1) The fluid mechanics of the circulation lag (delay) for a three-dimensional wing needs to be identified. Although many of these parameters have been qualitatively investigated, the influence of wing span, airfoil section, tip design, boundary layer separation, global rotation rates, localized time dependent rotation rates, pivot point, wing sweep, wing dihedral, Mach number, and Reynolds number need to be quantitatively measured accompanied by appropriate theories.

(2) The flow field for these cases needs to be visualized and a clear explanation of the vortex structure needs to be documented.

(3) The mechanics of the downwash associated with oscillating configurations needs to be investigated quantitatively and the structure of the downwash field should be clearly described.

(4) The coupling between the circulation lag on each wing and the downwash field should be investigated. Properties of the system which produce a shift in the downwash normal force curves and an accompanying upwash on an aft wing should be identified and investigated.

(5) Accurate wind tunnel test data for most of these previously described configurations is lacking and experimental tests need to be conducted to build a more extensive database.

(6) The problems associated with subscale testing and similarity matching for subscale tests needs to be further investigated and clearly documented.

REFERENCES

1. McAlister, Kenneth W.; Carr, Lawrence W.; and McCroskey, William J., "Dynamic Stall Experiments on the NACA 0012 Airfoil", NASA Technical Paper 1100, Ames Research Center, Moffett Field, CA., 1978

2. Carr, L. W., "Progress in Analysis and Prediction of Dynamic Stall," Journal of Aircraft, Vol.25, No. 1, Jan. 1988.

3. Albertson, J. A., Troutt, T. R., Siuru, W. D., and Walker, J. M., "Dynamic Stall Vortex Development and the Surface Pressure Field of a Pitching Airfoil," AIAA Paper 87-1333, AIAA 19th Fluid Dynamics, Plasma Dynamics and Lasers Conference, Honolulu, Hawaii, 1987.

4. Stephen, E., Walker, J., Roh, J., Eldred, T., and Beals, M., "Extended Pitch Axis Effects on the Flow about Pitching Airfoils," AIAA Paper 89-0025, AIAA 27th Aerospace Sciences Meeting, Reno NV 1989.

5. Robinson, M., Walker, J., Wissler, J., "Unsteady Surface Pressure Measurements on a Pitching Rectangular Wing," Proceedings: Workshop II on Unsteady Separated Flow, FJSRL-TR-88-0004, Sept. 1988, pp 225-237.

6. Ericsson, L. E., and Reding, J. P., "Fluid Mechanics of Dynamic Stall, Part I. Unsteady Flow Concepts," Journal of Fluids and Structures, Vol. 2, 1988, pp 1-33.

7. Ericsson, L. E., and Reding, J. P., "Fluid Mechanics of Dynamic Stall, Part II. Prediction of Full-Scale Characteristics," Journal of Fluids and Structures, Vol. 2, 1988, pp 113-143.

8. den Boer, R. G. and Cunningham, A. M. Jr., "Low Speed Unsteady Aerodynamics of a Pitched Straked Wing at High Incidence - Part I: Test Program," Journal of Aircraft, Vol. 27, No.1, Jan. 1990, pp 23-30.

9. Cunningham, A. M. Jr., and den Boer, R. G., "Low Speed Unsteady Aerodynamics of a Pitched Straked Wing at High Incidence - Part II: Harmonic Analysis," Journal of Aircraft, Vol. 27, No.1, Jan. 1990, pp 31-41.

10. Ericsson, L. E., and Reding, J. P., "Dynamic Support Interference in High Alpha Testing," Journal of Aircraft, Vol. 23, No. 12., Dec. 1986, pp 889-896.

11. Katz, J. and Maskew, B., "Unsteady Low Speed Aerodynamic Model for Complete Aircraft Configurations," Journal of Aircraft, Vol. 25, No. 4, April 1988, pp 302-310.

12. Konstadinopoulos, P., Thrasher, D. F., Mook, D. T., Nayfeh, A. H. and Watson, L., "A Vortex-Lattice Method for General, Unsteady Aerodynamics", Journal of Aircraft, Vol. 22, No. 1., Jan. 1985, pp 43-49.

13. Ashworth, J., Mouch, T. and Luttges, M., "Application of Forced Unsteady Aerodynamics to a Forward Swept Wing X-29 Model," AIAA Paper 88-0563, AIAA 29th Aerospace Sciences Meeting, Reno, NV. 1988.

14. Ashworth, J., Crisler, W., and Luttges, M., "Vortex Flows Created by Sinusoidal Oscillation of Three-Dimensional Wings," AIAA Paper 89-2227, AIAA 7th Applied Aerodynamics Conference, Seattle, WA. 1989.

15. Ohmi,K., Coutanceau, M., Daube, O., and Ta Phuloc Loc, "Further Experiments on Vortex Formation Around an Oscillating and Translating Airfoil at Large Incidences", Journal of Fluid Mechanics, Vol. 225, April 1991, pp 607-630.

16. Ohmi,K., Coutanceau, M., Ta Phuloc Loc and Dulieu, "Vortex Formation Around an Oscillating and Translating Airfoil at Large Incidences", Journal of Fluid Mechanics, Vol. 211, Feb. 1990, pp 37-60.

17. Visbal, M. R., and Shang, J. S., "Investigation of the Flow Structure Around a Rapidly Pitching Airfoil," AIAA Journal, Vol. 27, No. 8, Aug. 1989, pp 1044-1051.

18. Walker, J., "Dynamic Stall Wake Interaction with a Trailing Airfoil," AIAA Paper 87-0239, AIAA 25th Aerospace Sciences Meeting, Reno NV 1987.

19. Cook, Richard J., "Similarity Conditions for Flows about Pitching Airfoils," Frank J. Seiler Research Lab, FJSRL-TM-87-0003, June 1987.

20. Helin, H. E. and Walker, J. M., "Interrelated Effects of Pitch Rate and Pivot on Airfoil Dynamic Stall," AIAA Paper 85-0130, 1985.

Appendix

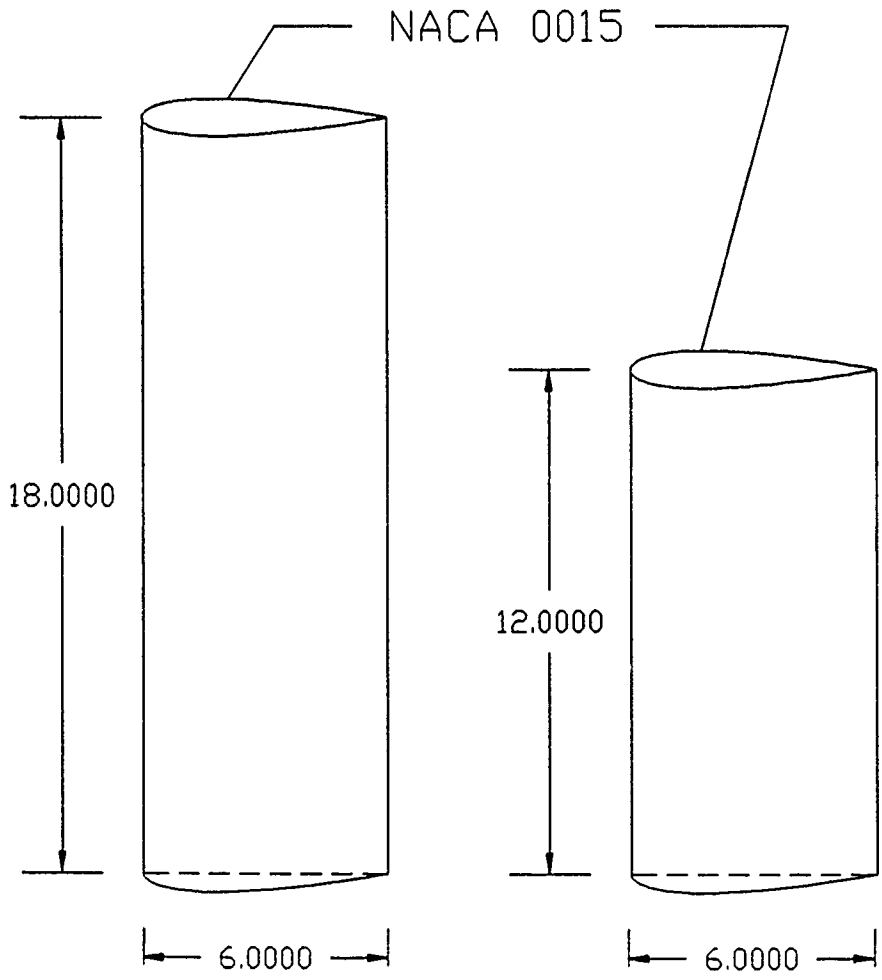

SCHEMATIC OF WINGS

RUN SCHEDULE COMPLETED

RUN #	CONFIG NUMB	ALPHA FWD	ALPHA AFT	DIHED FWD	DIHED AFT	SPECIAL (1)	NOTES (2)	WING SEP	ROT RATE
0800	WA1	0	-31	0	0	300	300	0	0
0801	WA1	0	-25	0	0	300	300	0	0
0802	WA1	0	-20	0	0	300	300	0	0
0803	WA1	0	-15	0	0	300	300	0	0
0804	WA1	0	-11	0	0	300	300	0	0
0805	WA1	0	-5	0	0	300	300	0	0
0806	WA1	0	0	0	0	300	300	0	0
0807	WA1	0	4	0	0	300	300	0	0
0808	WA1	0	10	0	0	300	300	0	0
0809	WA1	0	15	0	0	300	300	0	0
0810	WA1	0	19	0	0	300	300	0	0
0811	WA1	0	23	0	0	300	300	0	0
0812	WF1	-30	0	0	0	300	300	0	0
0813	WF1	-25	0	0	0	300	300	0	0
0814	WF1	-20	0	0	0	300	300	0	0
0815	WF1	-16	0	0	0	300	300	0	0
0816	WF1	-10	0	0	0	300	300	0	0
0817	WF1	-5	0	0	0	300	300	0	0
0818	WF1	0	0	0	0	300	300	0	0
0819	WF1	5	0	0	0	300	300	0	0
0820	WF1	10	0	0	0	300	300	0	0
0821	WF1	15	0	0	0	300	300	0	0
0822	WF1	19	0	0	0	300	300	0	0
0823	WF1	23	0	0	0	300	300	0	0
0824	WA2	0	-30	0	0	300	300	0	0
0825	WA2	0	-25	0	0	300	300	0	0
0826	WA2	0	-19	0	0	300	300	0	0
0827	WA2	0	-15	0	0	300	300	0	0
0828	WA2	0	-10	0	0	300	300	0	0
0829	WA2	0	-5	0	0	300	300	0	0
0830	WA2	0	0	0	0	300	300	0	0
0831	WA2	0	5	0	0	300	300	0	0
0832	WA2	0	10	0	0	300	300	0	0
0833	WA2	0	15	0	0	300	300	0	0
0834	WA2	0	21	0	0	300	300	0	0
0835	WA2	0	24	0	0	300	300	0	0
0836	WF2	-31	0	0	0	300	300	0	0
0837	WF2	-25	0	0	0	300	300	0	0
0838	WF2	-20	0	0	0	300	300	0	0
0839	WF2	-15	0	0	0	300	300	0	0
0840	WF2	-10	0	0	0	300	300	0	0
0841	WF2	-5	0	0	0	300	300	0	0
0842	WF2	0	0	0	0	300	300	0	0
0843	WF2	5	0	0	0	300	300	0	0
0844	WF2	9	0	0	0	300	300	0	0
0845	WF2	15	0	0	0	300	300	0	0
0846	WF2	20	0	0	0	300	300	0	0
0847	WF2	23	0	0	0	300	300	0	0
0848	WA1	0	999	0	0	800	811	0	0
0849	WF1	999	0	0	0	812	823	0	0
0850	WA2	0	999	0	0	824	835	0	0
0851	WF2	999	0	0	0	836	847	0	0

RUN SCHEDULE - CONTINUED

RUN #	CONFIG NUMB	ALPHA FWD	ALPHA AFT	DIHED FWD	DIHED AFT	SPECIAL (1)	NOTES (2)	WING SEP	ROT RATE
0852	WA1	999	-37	0	10	300	300	0	0
0853	WA1	999	-31	0	10	300	300	0	0
0854	WA1	999	-27	0	10	300	300	0	0
0855	WA1	999	-21	0	10	300	300	0	0
0856	WA1	999	-15	0	10	300	300	0	0
0857	WA1	999	-11	0	10	300	300	0	0
0858	WA1	999	-3	0	10	300	300	0	0
0859	WA1	999	3	0	10	300	300	0	0
0860	WA1	999	10	0	10	300	300	0	0
0861	WA1	999	15	0	10	300	300	0	0
0862	WA1	999	20	0	10	300	300	0	0
0863	WA1	999	23	0	10	300	300	0	0
0864	WA1	999	0	0	10	852	863	0	0
0865	WA1WF1	-38	-38	-10	10	0	0	0	0
0866	WA1WF1	-30	-30	-10	10	0	0	0	0
0867	WA1WF1	-23	-23	-10	10	0	0	0	0
0868	WA1WF1	-15	-15	-10	10	0	0	0	0
0869	WA1WF1	-9	-9	-10	10	0	0	0	0
0870	WA1WF1	-3	-3	-10	10	0	0	0	0
0871	WA1WF1	2	2	-10	10	0	0	0	0
0872	WA1WF1	7	7	-10	10	0	0	0	0
0873	WA1WF1	11	11	-10	10	0	0	0	0
0874	WA1WF1	16	16	-10	10	0	0	0	0
0875	WA1WF1	19	19	-10	10	0	0	0	0
0876	WA1WF1	23	23	-10	10	0	0	0	0
0877	WA1WF1	0	0	-10	10	865	876	0	0
0878	WA1WF1	-38	[illegible]	0	10	0	0	0	0
0879	WA1WF1	-29	-29	0	10	0	0	0	0
0880	WA1WF1	-23	-23	0	10	0	0	0	0
0881	WA1WF1	-15	-15	0	10	0	0	0	0
0882	WA1WF1	-12	-12	0	10	0	0	0	0
0883	WA1WF1	-4	-4	0	10	0	0	0	0
0884	WA1WF1	2	2	0	10	0	0	0	0
0885	WA1WF1	8	8	0	10	0	0	0	0
0886	WA1WF1	13	13	0	10	0	0	0	0
0887	WA1WF1	18	18	0	10	0	0	0	0
0888	WA1WF1	20	20	0	10	0	0	0	0
0889	WA1WF1	23	23	0	10	0	0	0	0
0890	WA1WF1	0	0	0	10	878	889	0	0

RUN SCHEDULE - CONTINUED

RUN #	CONFIG NUMB	ALPHA FWD	ALPHA AFT	DIHED FWD	DIHED AFT	SPECIAL (1)	NOTES (2)	WING SEP	ROT RATE
0900	WA1WF2	-31	-31	0	0	300	300	0	0
0901	WA1WF2	-25	-25	0	0	300	300	0	0
0902	WA1WF2	-19	-19	0	0	300	300	0	0
0903	WA1WF2	-15	-15	0	0	300	300	0	0
0904	WA1WF2	-10	-10	0	0	300	300	0	0
0905	WA1WF2	-5	-5	0	0	300	300	0	0
0906	WA1WF2	0	0	0	0	300	300	0	0
0907	WA1WF2	5	5	0	0	300	300	0	0
0908	WA1WF2	10	10	0	0	300	300	0	0
0909	WA1WF2	15	15	0	0	300	300	0	0
0910	WA1WF2	21	21	0	0	300	300	0	0
0911	WA1WF2	26	26	0	0	300	300	0	0
0920	WA1WF1	-30	-30	0	0	300	300	0	0
0921	WA1WF1	-25	-25	0	0	300	300	0	0
0922	WA1WF1	-20	-20	0	0	300	300	0	0
0923	WA1WF1	-15	-15	0	0	300	300	0	0
0924	WA1WF1	-10	-10	0	0	300	300	0	0
0925	WA1WF1	-5	-5	0	0	300	300	0	0
0926	WA1WF1	0	0	0	0	300	300	0	0
0927	WA1WF1	5	5	0	0	300	300	0	0
0928	WA1WF1	9	9	0	0	300	300	0	0
0929	WA1WF1	14	14	0	0	300	300	0	0
0930	WA1WF1	19	19	0	0	300	300	0	0
0931	WA1WF1	23	23	0	0	300	300	0	0
0932	WA1WF1	26	26	0	0	300	300	0	0
0933	WA2WF1	-30	-30	0	0	300	300	0	0
0934	WA2WF1	-25	-25	0	0	300	300	0	0
0935	WA2WF1	-20	-20	0	0	300	300	0	0
0936	WA2WF1	-16	-16	0	0	300	300	0	0
0937	WA2WF1	-10	-10	0	0	300	300	0	0
0938	WA2WF1	-5	-5	0	0	300	300	0	0
0939	WA2WF1	0	0	0	0	300	300	0	0
0940	WA2WF1	4	4	0	0	300	300	0	0
0941	WA2WF1	9	9	0	0	300	300	0	0
0942	WA2WF1	15	15	0	0	300	300	0	0
0943	WA2WF1	19	19	0	0	300	300	0	0
0944	WA2WF1	25	25	0	0	300	300	0	0
0980	WA1WF2	999	999	0	0	900	911	0	0
0981	WA1WF1	999	999	0	0	920	932	0	0
0982	WA2WF1	999	999	0	0	933	944	0	0
0986	WA1WF1	0	0	0	0	1	504	0	10
0987	WA1WF1	0	0	0	0	1	517	0	20
0988	WA1WF1	0	0	0	0	1	530	0	40
0989	WA1WF1	0	0	0	0	1	699	1.067	10
0990	WA1WF1	0	0	0	0	1	712	1.067	25
0991	WA1WF1	0	0	0	0	1	725	2.127	10
0992	WA1WF1	0	0	0	0	1	738	2.127	25
0993	WA1WF1	0	0	0	0	1	751	3.171	10
0994	WA1WF1	0	0	0	0	1	764	3.171	25
0995	WA1WF1	0	0	0	0	1	855	-1.07	10
0996	WA1WF1	0	0	0	0	1	868	-1.07	25
0997	WA1WF1	0	0	0	0	1	881	-3.17	10
0998	WA1WF1	0	0	0	0	1	894	-3.17	25
0999	WA1WF2	0	0	0	0	1	998	-2.13	25

RUN SCHEDULE - CONTINUED

RUN #	CONFIG NUMB	ALPHA FWD	ALPHA AFT	DIHED FWD	DIHED AFT	SPECIAL (1)	NOTES (2)	WING SEP	ROT RATE
1000	WF1	0	999	0	999	0	999	999.9	10
1001	WF1	5	999	0	999	0	999	999.9	10
1002	WF1	10	999	0	999	0	999	999.9	10
1003	WF1	15	999	0	999	0	999	999.9	10
1004	WF1	-5	999	0	999	0	999	999.9	10
1005	WF1	-10	999	0	999	0	999	999.9	10
1006	WF1	-15	999	0	999	0	999	999.9	10
1014	WF1	0	999	-10	999	0	999	999.9	10
1015	WF1	5	999	-10	999	0	999	999.9	10
1016	WF1	10	999	-10	999	0	999	999.9	10
1017	WF1	15	999	-10	999	0	999	999.9	10
1018	WF1	-5	999	-10	999	0	999	999.9	10
1019	WF1	-10	999	-10	999	0	999	999.9	10
1020	WF1	-15	999	-10	999	0	999	999.9	10
1028	WF2	0	999	0	999	0	999	999.9	10
1029	WF2	5	999	0	999	0	999	999.9	10
1030	WF2	10	999	0	999	0	999	999.9	10
1031	WF2	15	999	0	999	0	999	999.9	10
1032	WF2	-5	999	0	999	0	999	999.9	10
1033	WF2	-10	999	0	999	0	999	999.9	10
1034	WF2	-15	999	0	999	0	999	999.9	10
1084	WF1	0	999	0	999	0	999	999.9	20
1085	WF1	5	999	0	999	0	999	999.9	20
1086	WF1	10	999	0	999	0	999	999.9	20
1087	WF1	15	999	0	999	0	999	999.9	20
1088	WF1	-5	999	0	999	0	999	999.9	20
1089	WF1	-10	999	0	999	0	999	999.9	20
1090	WF1	-15	999	0	999	0	999	999.9	20
1098	WF1	0	999	-10	999	0	999	999.9	20
1099	WF1	5	999	-10	999	0	999	999.9	20
1100	WF1	10	999	-10	999	0	999	999.9	20
1101	WF1	15	999	-10	999	0	999	999.9	20
1102	WF1	-5	999	-10	999	0	999	999.9	20
1103	WF1	-10	999	-10	999	0	999	999.9	20
1104	WF1	-15	999	-10	999	0	999	999.9	20
1112	WF2	0	999	0	999	0	999	999.9	20
1113	WF2	5	999	0	999	0	999	999.9	20
1114	WF2	10	999	0	999	0	999	999.9	20
1115	WF2	15	999	0	999	0	999	999.9	20
1116	WF2	-5	999	0	999	0	999	999.9	20
1117	WF2	-10	999	0	999	0	999	999.9	20
1118	WF2	-15	999	0	999	0	999	999.9	20
1168	WF1	0	999	0	999	0	999	999.9	40
1169	WF1	5	999	0	999	0	999	999.9	40
1170	WF1	10	999	0	999	0	999	999.9	40
1171	WF1	15	999	0	999	0	999	999.9	40
1172	WF1	-5	999	0	999	0	999	999.9	40
1173	WF1	-10	999	0	999	0	999	999.9	40
1174	WF1	-15	999	0	999	0	999	999.9	40
1182	WF1	0	999	-10	999	0	999	999.9	40
1183	WF1	5	999	-10	999	0	999	999.9	40
1184	WF1	10	999	-10	999	0	999	999.9	40
1185	WF1	15	999	-10	999	0	999	999.9	40
1186	WF1	-5	999	-10	999	0	999	999.9	40
1187	WF1	-10	999	-10	999	0	999	999.9	40
1188	WF1	-15	999	-10	999	0	999	999.9	40

RUN SCHEDULE - CONTINUED

RUN #	CONFIG NUMB	ALPHA FWD	ALPHA AFT	DIHED FWD	DIHED AFT	SPECIAL (1)	NOTES (2)	WING SEP	ROT RATE
1196	WF2	0	999	0	999	0	999	999.9	40
1197	WF2	5	999	0	999	0	999	999.9	40
1198	WF2	10	999	0	999	0	999	999.9	40
1199	WF2	15	999	0	999	0	999	999.9	40
1200	WF2	-5	999	0	999	0	999	999.9	40
1201	WF2	-10	999	0	999	0	999	999.9	40
1202	WF2	-15	999	0	999	0	999	999.9	40
1252	WA1	999	0	999	0	999	0	999.9	10
1253	WA1	999	5	999	0	999	0	999.9	10
1254	WA1	999	10	999	0	999	0	999.9	10
1255	WA1	999	15	999	0	999	0	999.9	10
1256	WA1	999	-5	999	0	999	0	999.9	10
1257	WA1	999	-10	999	0	999	0	999.9	10
1258	WA1	999	-15	999	0	999	0	999.9	10
1266	WA1	999	0	999	10	999	0	999.9	10
1267	WA1	999	5	999	10	999	0	999.9	10
1268	WA1	999	10	999	10	999	0	999.9	10
1269	WA1	999	15	999	10	999	0	999.9	10
1270	WA1	999	-5	999	10	999	0	999.9	10
1280	WA1	999	0	999	0	999	0	999.9	20
1281	WA1	999	5	999	0	999	0	999.9	20
1282	WA1	999	10	999	0	999	0	999.9	20
1283	WA1	999	15	999	0	999	0	999.9	20
1284	WA1	999	-5	999	0	999	0	999.9	20
1285	WA1	999	-10	999	0	999	0	999.9	20
1286	WA1	999	-15	999	0	999	0	999.9	20
1294	WA1	999	0	999	10	999	0	999.9	20
1295	WA1	999	5	999	10	999	0	999.9	20
1296	WA1	999	10	999	10	999	0	999.9	20
1297	WA1	999	15	999	10	999	0	999.9	20
1298	WA1	999	-5	999	10	999	0	999.9	20
1308	WA1	999	0	999	0	999	0	999.9	40
1309	WA1	999	5	999	0	999	0	999.9	40
1310	WA1	999	10	999	0	999	0	999.9	40
1311	WA1	999	15	999	0	999	0	999.9	40
1312	WA1	999	-5	999	0	999	0	999.9	40
1313	WA1	999	-10	999	0	999	0	999.9	40
1314	WA1	999	-15	999	0	999	0	999.9	40
1322	WA1	999	0	999	10	999	0	999.9	40
1323	WA1	999	5	999	10	999	0	999.9	40
1324	WA1	999	10	999	10	999	0	999.9	40
1325	WA1	999	15	999	10	999	0	999.9	40
1326	WA1	999	-5	999	10	999	0	999.9	40
1336	WA2	999	0	999	0	999	0	999.9	10
1337	WA2	999	5	999	0	999	0	999.9	10
1338	WA2	999	10	999	0	999	0	999.9	10
1339	WA2	999	15	999	0	999	0	999.9	10
1340	WA2	999	-5	999	0	999	0	999.9	10
1341	WA2	999	-10	999	0	999	0	999.9	10
1342	WA2	999	-15	999	0	999	0	999.9	10
1350	WA2	999	0	999	10	999	0	999.9	10
1351	WA2	999	5	999	10	999	0	999.9	10
1352	WA2	999	10	999	10	999	0	999.9	10
1353	WA2	999	15	999	10	999	0	999.9	10
1354	WA2	999	-5	999	10	999	0	999.9	10

RUN SCHEDULE - CONTINUED

RUN #	CONFIG NUMB	ALPHA FWD	ALPHA AFT	DIHED FWD	DIHED AFT	SPECIAL (1)	NOTES (2)	WING SEP	ROT RATE
1364	WA2	999	0	999	0	999	0	999.9	20
1365	WA2	999	5	999	0	999	0	999.9	20
1366	WA2	999	10	999	0	999	0	999.9	20
1367	WA2	999	15	999	0	999	0	999.9	20
1368	WA2	999	-5	999	0	999	0	999.9	20
1369	WA2	999	-10	999	0	999	0	999.9	20
1370	WA2	999	-15	999	0	999	0	999.9	20
1378	WA2	999	0	999	10	999	0	999.9	20
1379	WA2	999	5	999	10	999	0	999.9	20
1380	WA2	999	10	999	10	999	0	999.9	20
1381	WA2	999	15	999	10	999	0	999.9	20
1382	WA2	999	-5	999	10	999	0	999.9	20
1392	WA2	999	0	999	0	999	0	999.9	40
1393	WA2	999	5	999	0	999	0	999.9	40
1394	WA2	999	10	999	0	999	0	999.9	40
1395	WA2	999	15	999	0	999	0	999.9	40
1396	WA2	999	-5	999	0	999	0	999.9	40
1397	WA2	999	-10	999	0	999	0	999.9	40
1398	WA2	999	-15	999	0	999	0	999.9	40
1406	WA2	999	0	999	10	999	0	999.9	40
1407	WA2	999	5	999	10	999	0	999.9	40
1408	WA2	999	10	999	10	999	0	999.9	40
1409	WA2	999	15	999	10	999	0	999.9	40
1410	WA2	999	-5	999	10	999	0	999.9	40
1504	WA1WF1	0	0	0	0	0	0	0	10
1505	WA1WF1	5	0	0	0	0	0	0	10
1506	WA1WF1	10	0	0	0	0	0	0	10
1507	WA1WF1	15	0	0	0	0	0	0	10
1508	WA1WF1	-5	0	0	0	0	0	0	10
1509	WA1WF1	-10	0	0	0	0	0	0	10
1510	WA1WF1	-15	0	0	0	0	0	0	10
1511	WA1WF1	0	5	0	0	0	0	0	10
1512	WA1WF1	0	10	0	0	0	0	0	10
1513	WA1WF1	0	15	0	0	0	0	0	10
1514	WA1WF1	0	-5	0	0	0	0	0	10
1515	WA1WF1	0	-10	0	0	0	0	0	10
1516	WA1WF1	0	-15	0	0	0	0	0	10
1517	WA1WF1	0	0	0	0	0	0	0	20
1518	WA1WF1	5	0	0	0	0	0	0	20
1519	WA1WF1	10	0	0	0	0	0	0	20
1520	WA1WF1	15	0	0	0	0	0	0	20
1521	WA1WF1	-5	0	0	0	0	0	0	20
1522	WA1WF1	-10	0	0	0	0	0	0	20
1523	WA1WF1	-15	0	0	0	0	0	0	20
1524	WA1WF1	0	5	0	0	0	0	0	20
1525	WA1WF1	0	10	0	0	0	0	0	--
1526	WA1WF1	0	15	0	0	0	0	0	20
1527	WA1WF1	0	-5	0	0	0	0	0	20
1528	WA1WF1	0	-10	0	0	0	0	0	20
1529	WA1WF1	0	-15	0	0	0	0	0	20
1530	WA1WF1	0	0	0	0	0	0	0	40
1531	WA1WF1	5	0	0	0	0	0	0	40
1532	WA1WF1	10	0	0	0	0	0	0	40
1533	WA1WF1	15	0	0	0	0	0	0	40
1534	WA1WF1	-5	0	0	0	0	0	0	40
1535	WA1WF1	-10	0	0	0	0	0	0	40
1536	WA1WF1	-15	0	0	0	0	0	0	40

RUN SCHEDULE - CONTINUED

RUN #	CONFIG NUMB	ALPHA FWD	ALPHA AFT	DIHED FWD	DIHED AFT	SPECIAL (1)	NOTES (2)	WING SEP	ROT RATE
1537	WA1WF1	0	5	0	0	0	0	0	40
1538	WA1WF1	0	10	0	0	0	0	0	40
1539	WA1WF1	0	15	0	0	0	0	0	40
1540	WA1WF1	0	-5	0	0	0	0	0	40
1541	WA1WF1	0	-10	0	0	0	0	0	40
1542	WA1WF1	0	-15	0	0	0	0	0	40
1595	WA1WF1	0	0	-10	10	0	0	0	10
1596	WA1WF1	5	0	-10	10	0	0	0	10
1597	WA1WF1	10	0	-10	10	0	0	0	10
1599	WA1WF1	-5	0	-10	10	0	0	0	10
1600	WA1WF1	-10	0	-10	10	0	0	0	10
1601	WA1WF1	-15	0	-10	10	0	0	0	10
1602	WA1WF1	0	5	-10	10	0	0	0	10
1603	WA1WF1	0	10	-10	10	0	0	0	10
1604	WA1WF1	0	15	-10	10	0	0	0	10
1605	WA1WF1	0	-5	-10	10	0	0	0	10
1608	WA1WF1	0	0	-10	10	0	0	0	25
1609	WA1WF1	5	0	-10	10	0	0	0	25
1610	WA1WF1	10	0	-10	10	0	0	0	25
1612	WA1WF1	-5	0	-10	10	0	0	0	25
1613	WA1WF1	-10	0	-10	10	0	0	0	25
1614	WA1WF1	-15	0	-10	10	0	0	0	25
1615	WA1WF1	0	5	-10	10	0	0	0	25
1616	WA1WF1	0	10	-10	10	0	0	0	25
1617	WA1WF1	0	15	-10	10	0	0	0	25
1618	WA1WF1	0	-5	-10	10	0	0	0	25
1621	WA1WF1	0	0	10	-10	0	0	0	10
1622	WA1WF1	5	0	10	-10	0	0	0	10
1623	WA1WF1	10	0	10	-10	0	0	0	10
1624	WA1WF1	15	0	10	-10	0	0	0	10
1625	WA1WF1	-5	0	10	-10	0	0	0	10
1628	WA1WF1	0	5	10	-10	0	0	0	10
1631	WA1WF1	0	-5	10	-10	0	0	0	10
1632	WA1WF1	0	-10	10	-10	0	0	0	10
1633	WA1WF1	0	-15	10	-10	0	0	0	10
1634	WA1WF1	0	0	10	-10	0	0	0	25
1635	WA1WF1	5	0	10	-10	0	0	0	25
1636	WA1WF1	10	0	10	-10	0	0	0	25
1637	WA1WF1	15	0	10	-10	0	0	0	25
1638	WA1WF1	-5	0	10	-10	0	0	0	25
1641	WA1WF1	0	5	10	-10	0	0	0	25
1644	WA1WF1	0	-5	10	-10	0	0	0	25
1645	WA1WF1	0	-10	10	-10	0	0	0	25
1646	WA1WF1	0	-15	10	-10	0	0	0	25
1699	WA1WF1	0	0	0	0	0	0	1.067	10
1700	WA1WF1	5	0	0	0	0	0	1.067	10
1701	WA1WF1	10	0	0	0	0	0	1.067	10
1702	WA1WF1	15	0	0	0	0	0	1.067	10
1703	WA1WF1	-5	0	0	0	0	0	1.067	10
1704	WA1WF1	-10	0	0	0	0	0	1.067	10
1705	WA1WF1	-15	0	0	0	0	0	1.067	10
1706	WA1WF1	0	5	0	0	0	0	1.067	10
1707	WA1WF1	0	10	0	0	0	0	1.067	10
1708	WA1WF1	0	15	0	0	0	0	1.067	10
1709	WA1WF1	0	-5	0	0	0	0	1.067	10
1710	WA1WF1	0	-10	0	0	0	0	1.067	10
1711	WA1WF1	0	-15	0	0	0	0	1.067	10

RUN SCHEDULE - CONTINUED

RUN #	CONFIG NUMB	ALPHA FWD	ALPHA AFT	DIHED FWD	DIHED AFT	SPECIAL (1)	NOTES (2)	WING SEP	ROT RATE
1712	WA1WF1	0	0	0	0	0	0	1.067	25
1713	WA1WF1	5	0	0	0	0	0	1.067	25
1714	WA1WF1	10	0	0	0	0	0	1.067	25
1715	WA1WF1	15	0	0	0	0	0	1.067	25
1716	WA1WF1	-5	0	0	0	0	0	1.067	25
1717	WA1WF1	-10	0	0	0	0	0	1.067	25
1718	WA1WF1	-15	0	0	0	0	0	1.067	25
1719	WA1WF1	0	5	0	0	0	0	1.067	25
1720	WA1WF1	0	10	0	0	0	0	1.067	25
1721	WA1WF1	0	15	0	0	0	0	1.067	25
1722	WA1WF1	0	-5	0	0	0	0	1.067	25
1723	WA1WF1	0	-10	0	0	0	0	1.067	25
1724	WA1WF1	0	-15	0	0	0	0	1.067	25
1725	WA1WF1	0	0	0	0	0	0	2.127	10
1726	WA1WF1	5	0	0	0	0	0	2.127	10
1727	WA1WF1	10	0	0	0	0	0	2.127	10
1728	WA1WF1	15	0	0	0	0	0	2.127	10
1729	WA1WF1	-5	0	0	0	0	0	2.127	10
1730	WA1WF1	-10	0	0	0	0	0	2.127	10
1731	WA1WF1	-15	0	0	0	0	0	2.127	10
1732	WA1WF1	0	5	0	0	0	0	2.127	10
1733	WA1WF1	0	10	0	0	0	0	2.127	10
1734	WA1WF1	0	15	0	0	0	0	2.127	10
1735	WA1WF1	0	-5	0	0	0	0	2.127	10
1736	WA1WF1	0	-10	0	0	0	0	2.127	10
1737	WA1WF1	0	-15	0	0	0	0	2.127	10
1738	WA1WF1	0	0	0	0	0	0	2.127	25
1739	WA1WF1	5	0	0	0	0	0	2.127	25
1740	WA1WF1	10	0	0	0	0	0	2.127	25
1741	WA1WF1	15	0	0	0	0	0	2.127	25
1742	WA1WF1	-5	0	0	0	0	0	2.127	25
1743	WA1WF1	-10	0	0	0	0	0	2.127	25
1744	WA1WF1	-15	0	0	0	0	0	2.127	25
1745	WA1WF1	0	5	0	0	0	0	2.127	25
1746	WA1WF1	0	10	0	0	0	0	2.127	25
1747	WA1WF1	0	15	0	0	0	0	2.127	25
1748	WA1WF1	0	-5	0	0	0	0	2.127	25
1749	WA1WF1	0	-10	0	0	0	0	2.127	25
1750	WA1WF1	0	-15	0	0	0	0	2.127	25
1751	WA1WF1	0	0	0	0	0	0	3.171	10
1752	WA1WF1	5	0	0	0	0	0	3.171	10
1753	WA1WF1	10	0	0	0	0	0	3.171	10
1754	WA1WF1	15	0	0	0	0	0	3.171	10
1755	WA1WF1	-5	0	0	0	0	0	3.171	10
1756	WA1WF1	-10	0	0	0	0	0	3.171	10
1757	WA1WF1	-15	0	0	0	0	0	3.171	10
1758	WA1WF1	0	5	0	0	0	0	3.171	10
1759	WA1WF1	0	10	0	0	0	0	3.171	10
1760	WA1WF1	0	15	0	0	0	0	3.171	10
1761	WA1WF1	0	-5	0	0	0	0	3.171	10
1762	WA1WF1	0	-10	0	0	0	0	3.171	10
1763	WA1WF1	0	-15	0	0	0	0	3.171	10

RUN SCHEDULE - CONTINUED

RUN #	CONFIG NUMB	ALPHA FWD	ALPHA AFT	DIHED FWD	DIHED AFT	SPECIAL (1)	NOTES (2)	WING SEP	ROT RATE
1764	WA1WF1	0	0	0	0	0	0	3.171	25
1765	WA1WF1	5	0	0	0	0	0	3.171	25
1766	WA1WF1	10	0	0	0	0	0	3.171	25
1767	WA1WF1	15	0	0	0	0	0	3.171	25
1768	WA1WF1	-5	0	0	0	0	0	3.171	25
1769	WA1WF1	-10	0	0	0	0	0	3.171	25
1770	WA1WF1	-15	0	0	0	0	0	3.171	25
1771	WA1WF1	0	5	0	0	0	0	3.171	25
1772	WA1WF1	0	10	0	0	0	0	3.171	25
1773	WA1WF1	0	15	0	0	0	0	3.171	25
1774	WA1WF1	0	-5	0	0	0	0	3.171	25
1775	WA1WF1	0	-10	0	0	0	0	3.171	25
1776	WA1WF1	0	-15	0	0	0	0	3.171	25
1855	WA1WF1	0	0	0	0	0	0	-1.07	10
1856	WA1WF1	5	0	0	0	0	0	-1.07	10
1857	WA1WF1	10	0	0	0	0	0	-1.07	10
1858	WA1WF1	15	0	0	0	0	0	-1.07	10
1859	WA1WF1	-5	0	0	0	0	0	-1.07	10
1860	WA1WF1	-10	0	0	0	0	0	-1.07	10
1861	WA1WF1	-15	0	0	0	0	0	-1.07	10
1862	WA1WF1	0	5	0	0	0	0	-1.07	10
1863	WA1WF1	0	10	0	0	0	0	-1.07	10
1864	WA1WF1	0	15	0	0	0	0	-1.07	10
1865	WA1WF1	0	-5	0	0	0	0	-1.07	10
1866	WA1WF1	0	-10	0	0	0	0	-1.07	10
1867	WA1WF1	0	-15	0	0	0	0	-1.07	10
1868	WA1WF1	0	0	0	0	0	0	-1.07	25
1869	WA1WF1	5	0	0	0	0	0	-1.07	25
1870	WA1WF1	10	0	0	0	0	0	-1.07	25
1871	WA1WF1	15	0	0	0	0	0	-1.07	25
1872	WA1WF1	-5	0	0	0	0	0	-1.07	25
1873	WA1WF1	-10	0	0	0	0	0	-1.07	25
1874	WA1WF1	-15	0	0	0	0	0	-1.07	25
1875	WA1WF1	0	5	0	0	0	0	-1.07	25
1876	WA1WF1	0	10	0	0	0	0	-1.07	25
1877	WA1WF1	0	15	0	0	0	0	-1.07	25
1878	WA1WF1	0	-5	0	0	0	0	-1.07	25
1879	WA1WF1	0	-10	0	0	0	0	-1.07	25
1880	WA1WF1	0	-15	0	0	0	0	-1.07	25
1881	WA1WF1	0	0	0	0	0	0	-3.17	10
1882	WA1WF1	5	0	0	0	0	0	-3.17	10
1883	WA1WF1	10	0	0	0	0	0	-3.17	10
1884	WA1WF1	15	0	0	0	0	0	-3.17	10
1885	WA1WF1	-5	0	0	0	0	0	-3.17	10
1886	WA1WF1	-10	0	0	0	0	0	-3.17	10
1887	WA1WF1	-15	0	0	0	0	0	-3.17	10
1888	WA1WF1	0	5	0	0	0	0	-3.17	10
1889	WA1WF1	0	10	0	0	0	0	-3.17	10
1890	WA1WF1	0	15	0	0	0	0	-3.17	10
1891	WA1WF1	0	-5	0	0	0	0	-3.17	10
1892	WA1WF1	0	-10	0	0	0	0	-3.17	10
1893	WA1WF1	0	-15	0	0	0	0	-3.17	10

RUN SCHEDULE - CONTINUED

RUN #	CONFIG NUMB	ALPHA FWD	ALPHA AFT	DIHED FWD	DIHED AFT	SPECIAL (1)	NOTES (2)	WING SEP	ROT RATE
1894	WA1WF1	0	0	0	0	0	0	-3.17	25
1895	WA1WF1	5	0	0	0	0	0	-3.17	25
1896	WA1WF1	10	0	0	0	0	0	-3.17	25
1897	WA1WF1	15	0	0	0	0	0	-3.17	25
1898	WA1WF1	-5	0	0	0	0	0	-3.17	25
1899	WA1WF1	-10	0	0	0	0	0	-3.17	25
1900	WA1WF1	-15	0	0	0	0	0	-3.17	25
1901	WA1WF1	0	5	0	0	0	0	-3.17	25
1902	WA1WF1	0	10	0	0	0	0	-3.17	25
1903	WA1WF1	0	15	0	0	0	0	-3.17	25
1904	WA1WF1	0	-5	0	0	0	0	-3.17	25
1905	WA1WF1	0	-10	0	0	0	0	-3.17	25
1906	WA1WF1	0	-15	0	0	0	0	-3.17	25
1933	WA1WF2	0	0	0	0	0	0	0	10
1934	WA1WF2	5	0	0	0	0	0	0	10
1935	WA1WF2	10	0	0	0	0	0	0	10
1936	WA1WF2	15	0	0	0	0	0	0	10
1937	WA1WF2	-5	0	0	0	0	0	0	10
1938	WA1WF2	-10	0	0	0	0	0	0	10
1939	WA1WF2	-15	0	0	0	0	0	0	10
1940	WA1WF2	0	5	0	0	0	0	0	10
1941	WA1WF2	0	10	0	0	0	0	0	10
1942	WA1WF2	0	15	0	0	0	0	0	10
1943	WA1WF2	0	-5	0	0	0	0	0	10
1944	WA1WF2	0	-10	0	0	0	0	0	10
1945	WA1WF2	0	-15	0	0	0	0	0	10
1946	WA1WF2	0	0	0	0	0	0	0	25
1947	WA1WF2	5	0	0	0	0	0	0	25
1948	WA1WF2	10	0	0	0	0	0	0	25
1949	WA1WF2	15	0	0	0	0	0	0	25
1950	WA1WF2	-5	0	0	0	0	0	0	25
1951	WA1WF2	-10	0	0	0	0	0	0	25
1952	WA1WF2	-15	0	0	0	0	0	0	25
1953	WA1WF2	0	5	0	0	0	0	0	25
1954	WA1WF2	0	10	0	0	0	0	0	25
1955	WA1WF2	0	15	0	0	0	0	0	25
1956	WA1WF2	0	-5	0	0	0	0	0	25
1957	WA1WF2	0	-10	0	0	0	0	0	25
1958	WA1WF2	0	-15	0	0	0	0	0	25
1959	WA1WF2	0	0	0	0	0	0	2.127	10
1960	WA1WF2	5	0	0	0	0	0	2.127	10
1961	WA1WF2	10	0	0	0	0	0	2.127	10
1962	WA1WF2	15	0	0	0	0	0	2.127	10
1963	WA1WF2	-5	0	0	0	0	0	2.127	10
1964	WA1WF2	-10	0	0	0	0	0	2.127	10
1965	WA1WF2	-15	0	0	0	0	0	2.127	10
1966	WA1WF2	0	5	0	0	0	0	2.127	10
1967	WA1WF2	0	10	0	0	0	0	2.127	10
1968	WA1WF2	0	15	0	0	0	0	2.127	10
1969	WA1WF2	0	-5	0	0	0	0	2.127	10
1970	WA1WF2	0	-10	0	0	0	0	2.127	10
1971	WA1WF2	0	-15	0	0	0	0	2.127	10

RUN SCHEDULE - CONTINUED

RUN #	CONFIG NUMB	ALPHA FWD	ALPHA AFT	DIHED FWD	DIHED AFT	SPECIAL (1)	NOTES (2)	WING SEP	ROT RATE
1972	WA1WF2	0	0	0	0	0	0	2.127	25
1973	WA1WF2	5	0	0	0	0	0	2.127	25
1974	WA1WF2	10	0	0	0	0	0	2.127	25
1975	WA1WF2	15	0	0	0	0	0	2.127	25
1976	WA1WF2	-5	0	0	0	0	0	2.127	25
1977	WA1WF2	-10	0	0	0	0	0	2.127	25
1978	WA1WF2	-15	0	0	0	0	0	2.127	25
1979	WA1WF2	0	5	0	0	0	0	2.127	25
1980	WA1WF2	0	10	0	0	0	0	2.127	25
1981	WA1WF2	0	15	0	0	0	0	2.127	25
1982	WA1WF2	0	-5	0	0	0	0	2.127	25
1983	WA1WF2	0	-10	0	0	0	0	2.127	25
1984	WA1WF2	0	-15	0	0	0	0	2.127	25
1985	WA1WF2	0	0	0	0	0	0	-2.13	10
1986	WA1WF2	5	0	0	0	0	0	-2.13	10
1987	WA1WF2	10	0	0	0	0	0	-2.13	10
1988	WA1WF2	15	0	0	0	0	0	-2.13	10
1989	WA1WF2	-5	0	0	0	0	0	-2.13	10
1990	WA1WF2	-10	0	0	0	0	0	-2.13	10
1991	WA1WF2	-15	0	0	0	0	0	-2.13	10
1992	WA1WF2	0	5	0	0	0	0	-2.13	10
1993	WA1WF2	0	10	0	0	0	0	-2.13	10
1994	WA1WF2	0	15	0	0	0	0	-2.13	10
1995	WA1WF2	0	-5	0	0	0	0	-2.13	10
1996	WA1WF2	0	-10	0	0	0	0	-2.13	10
1997	WA1WF2	0	-15	0	0	0	0	-2.13	10
1998	WA1WF2	0	0	0	0	0	0	-2.13	25
1999	WA1WF2	5	0	0	0	0	0	-2.13	25
2000	WA1WF2	10	0	0	0	0	0	-2.13	25
2001	WA1WF2	15	0	0	0	0	0	-2.13	25
2002	WA1WF2	-5	0	0	0	0	0	-2.13	25
2003	WA1WF2	-10	0	0	0	0	0	-2.13	25
2004	WA1WF2	-15	0	0	0	0	0	-2.13	25
2005	WA1WF2	0	5	0	0	0	0	-2.13	25
2006	WA1WF2	0	10	0	0	0	0	-2.13	25
2007	WA1WF2	0	15	0	0	0	0	-2.13	25
2008	WA1WF2	0	-5	0	0	0	0	-2.13	25
2009	WA1WF2	0	-10	0	0	0	0	-2.13	25
2010	WA1WF2	0	-15	0	0	0	0	-2.13	25
2089	WA2WF1	0	0	0	0	0	0	0	10
2090	WA2WF1	5	0	0	0	0	0	0	10
2091	WA2WF1	10	0	0	0	0	0	0	10
2092	WA2WF1	15	0	0	0	0	0	0	10
2093	WA2WF1	-5	0	0	0	0	0	0	10
2094	WA2WF1	-10	0	0	0	0	0	0	10
2095	WA2WF1	-15	0	0	0	0	0	0	10
2096	WA2WF1	0	5	0	0	0	0	0	10
2097	WA2WF1	0	10	0	0	0	0	0	10
2098	WA2WF1	0	15	0	0	0	0	0	10
2099	WA2WF1	0	-5	0	0	0	0	0	10
2100	WA2WF1	0	-10	0	0	0	0	0	10
2101	WA2WF1	0	-15	0	0	0	0	0	10

RUN SCHEDULE - CONTINUED

RUN #	CONFIG NUMB	ALPHA FWD	ALPHA AFT	DIHED FWD	DIHED AFT	SPECIAL (1)	NOTES (2)	WING SEP	ROT RATE
2102	WA2WF1	0	0	0	0	0	0	0	25
2103	WA2WF1	5	0	0	0	0	0	0	25
2104	WA2WF1	10	0	0	0	0	0	0	25
2105	WA2WF1	15	0	0	0	0	0	0	25
2106	WA2WF1	-5	0	0	0	0	0	0	25
2107	WA2WF1	-10	0	0	0	0	0	0	25
2108	WA2WF1	-15	0	0	0	0	0	0	25
2109	WA2WF1	0	5	0	0	0	0	0	25
2110	WA2WF1	0	10	0	0	0	0	0	25
2111	WA2WF1	0	15	0	0	0	0	0	25
2112	WA2WF1	0	-5	0	0	0	0	0	25
2113	WA2WF1	0	-10	0	0	0	0	0	25
2114	WA2WF1	0	-15	0	0	0	0	0	25
2115	WA2WF1	0	0	0	0	0	0	2.127	10
2116	WA2WF1	5	0	0	0	0	0	2.127	10
2117	WA2WF1	10	0	0	0	0	0	2.127	10
2118	WA2WF1	15	0	0	0	0	0	2.127	10
2119	WA2WF1	-5	0	0	0	0	0	2.127	10
2120	WA2WF1	-10	0	0	0	0	0	2.127	10
2121	WA2WF1	-15	0	0	0	0	0	2.127	10
2122	WA2WF1	0	5	0	0	0	0	2.127	10
2123	WA2WF1	0	10	0	0	0	0	2.127	10
2124	WA2WF1	0	15	0	0	0	0	2.127	10
2125	WA2WF1	0	-5	0	0	0	0	2.127	10
2126	WA2WF1	0	-10	0	0	0	0	2.127	10
2127	WA2WF1	0	-15	0	0	0	0	2.127	10
2128	WA2WF1	0	0	0	0	0	0	2.127	25
2129	WA2WF1	5	0	0	0	0	0	2.127	25
2130	WA2WF1	10	0	0	0	0	0	2.127	25
2131	WA2WF1	15	0	0	0	0	0	2.127	25
2132	WA2WF1	-5	0	0	0	0	0	2.127	25
2133	WA2WF1	-10	0	0	0	0	0	2.127	25
2134	WA2WF1	-15	0	0	0	0	0	2.127	25
2135	WA2WF1	0	5	0	0	0	0	2.127	25
2136	WA2WF1	0	10	0	0	0	0	2.127	25
2137	WA2WF1	0	15	0	0	0	0	2.127	25
2138	WA2WF1	0	-5	0	0	0	0	2.127	25
2139	WA2WF1	0	-10	0	0	0	0	2.127	25
2140	WA2WF1	0	-15	0	0	0	0	2.127	25
2141	WA2WF1	0	0	0	0	0	0	-2.13	10
2142	WA2WF1	5	0	0	0	0	0	-2.13	10
2143	WA2WF1	10	0	0	0	0	0	-2.13	10
2144	WA2WF1	15	0	0	0	0	0	-2.13	10
2145	WA2WF1	-5	0	0	0	0	0	-2.13	10
2146	WA2WF1	-10	0	0	0	0	0	-2.13	10
2147	WA2WF1	-15	0	0	0	0	0	-2.13	10
2148	WA2WF1	0	5	0	0	0	0	-2.13	10
2149	WA2WF1	0	10	0	0	0	0	-2.13	10
2150	WA2WF1	0	15	0	0	0	0	-2.13	10
2151	WA2WF1	0	-5	0	0	0	0	-2.13	10
2152	WA2WF1	0	-10	0	0	0	0	-2.13	10
2153	WA2WF1	0	-15	0	0	0	0	-2.13	10

RUN SCHEDULE - CONTINUED

RUN #	CONFIG NUMB	ALPHA FWD	ALPHA AFT	DIHED FWD	DIHED AFT	SPECIAL (1)	NOTES (2)	WING SEP	ROT RATE
2154	WA2WF1	0	0	0	0	0	0	-2.13	25
2155	WA2WF1	5	0	0	0	0	0	-2.13	25
2156	WA2WF1	10	0	0	0	0	0	-2.13	25
2157	WA2WF1	15	0	0	0	0	0	-2.13	25
2158	WA2WF1	-5	0	0	0	0	0	-2.13	25
2159	WA2WF1	-10	0	0	0	0	0	-2.13	25
2160	WA2WF1	-15	0	0	0	0	0	-2.13	25
2161	WA2WF1	0	5	0	0	0	0	-2.13	25
2162	WA2WF1	0	10	0	0	0	0	-2.13	25
2163	WA2WF1	0	15	0	0	0	0	-2.13	25
2164	WA2WF1	0	-5	0	0	0	0	-2.13	25
2165	WA2WF1	0	-10	0	0	0	0	-2.13	25
2166	WA2WF1	0	-15	0	0	0	0	-2.13	25
2245	WA2WF1	0	0	-10	10	0	0	0	10
2246	WA2WF1	5	0	-10	10	0	0	0	10
2247	WA2WF1	10	0	-10	10	0	0	0	10
2248	WA2WF1	15	0	-10	10	0	0	0	10
2249	WA2WF1	-5	0	-10	10	0	0	0	10
2250	WA2WF1	-10	0	-10	10	0	0	0	10
2251	WA2WF1	-15	0	-10	10	0	0	0	10
2252	WA2WF1	0	5	-10	10	0	0	0	10
2253	WA2WF1	0	10	-10	10	0	0	0	10
2254	WA2WF1	0	15	-10	10	0	0	0	10
2255	WA2WF1	0	-5	-10	10	0	0	0	10
2256	WA2WF1	0	-10	-10	10	0	0	0	10
2257	WA2WF1	0	-15	-10	10	0	0	0	10
2258	WA2WF1	0	0	-10	10	0	0	0	25
2259	WA2WF1	5	0	-10	10	0	0	0	25
2260	WA2WF1	10	0	-10	10	0	0	0	25
2261	WA2WF1	15	0	-10	10	0	0	0	25
2262	WA2WF1	-5	0	-10	10	0	0	0	25
2263	WA2WF1	-10	0	-10	10	0	0	0	25
2264	WA2WF1	-15	0	-10	10	0	0	0	25
2265	WA2WF1	0	5	-10	10	0	0	0	25
2266	WA2WF1	0	10	-10	10	0	0	0	25
2267	WA2WF1	0	15	-10	10	0	0	0	25
2268	WA2WF1	0	-5	-10	10	0	0	0	25